



Shank postsynaptic scaffolding proteins in autism spectrum disorder: Mouse models and their dysfunctions in behaviors, synapses, and molecules

Sunmin Jung^a, Mikyoung Park^{a,b,*}

^a Brain Science Institute, Korea Institute of Science and Technology, Seoul 02792, South Korea

^b Division of Bio-Medical Science & Technology, KIST School, Korea University of Science and Technology, Seoul 02792, South Korea

ARTICLE INFO

Keywords:

Postsynaptic scaffolding protein
Shank
Animal model
Autism spectrum disorder
Neurodevelopmental disorder
Psychiatric disorder

ABSTRACT

Postsynaptic scaffolding proteins, which are major components of the postsynaptic density (PSD) at excitatory synapses, include Shank, PSD-95, A-kinase anchoring protein, Homer, and SAP90/PSD-95-associated protein families and play crucial roles in synaptic structure, signaling, and functions. Several genetic studies have indicated that postsynaptic scaffolding proteins contribute to the etiology of various psychiatric disorders, including neurodevelopmental disorders. Indeed, mice with mutations or deletions in specific genes encoding postsynaptic scaffolding proteins display alterations in behavioral phenotypes that are relevant to specific psychiatric disorders. Here, we review recent studies on various mutant mouse models of Shank postsynaptic scaffolding proteins associated with autism spectrum disorder, a major neurodevelopmental disorder, and discuss future directions and therapeutic strategies for the treatment of autism spectrum disorder.

1. Introduction

Psychiatric disorders, also called mental disorders or mental illnesses, are health conditions that involve significant changes in thinking, emotion, and/or behavior, and are associated with abnormal functioning in social communication and interaction. Psychiatric disorders include neurodevelopmental disorders, such as autism spectrum disorder (ASD), schizophrenia, attention-deficit hyperactivity disorder (ADHD), Tourette's syndrome, obsessive-compulsive disorder, bipolar and related disorders, and anxiety disorders. Individuals with ASD have limited and repetitive behavioral patterns, as well as problems with social communication and interaction. ASD begins in early childhood, and its symptoms are often observed within the first year of life. As the word "spectrum" in its name indicates, ASD is associated with a vast range of symptoms and severity, and includes disorders such as autism, Asperger's syndrome, and Rett syndrome [1]. Each child with ASD has their own severity level, from normal to very severe, for each symptom. This feature of ASD endows each child with a unique mixture of symptoms, making ASD difficult to study, diagnose, and treat.

Synaptic molecules that are major components of the postsynaptic density (PSD), a huge complex containing thousands of proteins in excitatory synapses located on the tip of dendritic spines [2,3], are known to play important roles in many psychiatric disorders, including

ASD. Postsynaptic scaffolding proteins, such as PSD-95, A-kinase anchoring protein (AKAP) family, Homer, SAP90/PSD-95-associated protein (SAPAP)/guanylate kinase-associated protein (GKAP), and Src homology 3 (SH3) and multiple ankyrin repeat domain (Shank) families, are major components of PSD protein complexes and contribute to the synaptic structure, signaling, and function [1,4]. Importantly, large-scale genomic and microarray data obtained from individuals with psychiatric disorders, including ASD, have identified disruptive mutations in several genes encoding postsynaptic scaffolding proteins [5–11].

The etiology of psychiatric disorders, including ASD, can be investigated by generating mouse models with genetic mutations found in individuals with psychiatric disorders. Although mice with mutation(s) in risk genes display similar phenotypes relevant to psychiatric disorders, the detailed molecular and behavioral characteristics are different for each mutant mouse, even those with mutations in the same genes. Here, we review mice with mutant *Shank* genes, which are well-known risk genes for ASD, discuss the molecular, synaptic, and behavioral phenotypes of *Shank* mutant mice, and provide suggestions for future studies to better understand ASD.

2. Shank postsynaptic scaffolding proteins and ASD

According to estimates from the Autism and Developmental

* Corresponding author at: Brain Science Institute, Korea Institute of Science and Technology, Seoul 02792, South Korea.

E-mail addresses: mpark@kist.re.kr, mikyoungpark7@gmail.com (M. Park).

<https://doi.org/10.1016/j.phrs.2022.106340>

Received 23 May 2022; Received in revised form 29 June 2022; Accepted 30 June 2022

Available online 2 July 2022

1043-6618/© 2022 The Author(s). Published by Elsevier Ltd. This is an open access article under the CC BY-NC-ND license (<http://creativecommons.org/licenses/by-nc-nd/4.0/>).

Disabilities Monitoring (ADDM) Network program funded by the Centers for Disease Control and Prevention (CDC), ASD is the most prevalent neurodevelopmental disorder, affecting one out of 54 children aged 8 years in the United States [12]. ASD is clinically characterized by impaired social interaction, defective communication, and stereotyped behaviors such as repetitive behaviors [13,14]. Since ASD is typically diagnosed based on the behavior of individuals, the identification of genetic biomarkers is of crucial importance. Extensive genetic studies have identified several candidate genes involved in ASD. These include genes encoding the presynaptic plasma membrane proteins such as neurexin 1, neurexin 2, and neurexin 3 [15–17], postsynaptic cell-adhesion molecules such as neuroligin 1, neuroligin 3, and neuroligin 4 [18,19], which form trans-synaptic cell-adhesion complexes with presynaptic neurexins [20], and postsynaptic scaffolding proteins such as Shank1, Shank2, Shank3 [5, 21–28], and PSD-95 [29] (Fig. 1). Shank proteins are the most promising candidates among these molecules because individuals with ASD have been identified to have mutations in *Shank* genes [5, 10, 22, 23, 30–32]. Importantly, many genetic studies have strongly suggested that mutations or disruptions in the *Shank3* gene are highly penetrant monogenic risk factors for ASD [22,23,30]. In this section, we discuss *Shank* genes, their mutant mouse models, and their phenotypes relevant to ASD with respect to behavioral, synaptic structural and functional, biochemical, and molecular aspects.

2.1. Shank in patients with ASD

Shank proteins, also known as proline-rich synapse-associated proteins (ProSAPs), are master scaffolding proteins located at the PSD of glutamatergic synapses, where they play essential roles in synaptic development and function [33]. Shank proteins, including Shank1, Shank2, and Shank3, contain several domains, including ankyrin repeat domains, an SH3 domain, a PSD-95/Discs large/Zona occludens-1 (PDZ) domain, a proline-rich region, and a sterile alpha motif domain (Fig. 2). Shank proteins directly interact with many synaptic and signaling

molecules, including α -fodrin via its ankyrin repeat domains [34], glutamate receptor-interacting protein 1 (GRIP1) via its SH3 domain [35,36], SAPAP/GKAP via its PDZ domain [33,37], and Homer via its proline-rich region [38,39] (Fig. 1). In addition, Shank proteins indirectly interact with α -amino-3-hydroxy-5-methyl-4-isoxazolepropionic acid (AMPA) receptors with the accessory protein stargazin [40], which is anchored by the PSD-95-SAPAP/GKAP complex to the PDZ domain of the Shank protein [38], and with *N*-methyl-D-aspartate (NMDA) receptors anchored by the PSD-95-SAPAP/GKAP complex to the PDZ domain of the Shank protein [41] (Fig. 1). G-protein-coupled metabotropic glutamate receptors (mGluRs) bind to Homer, which directly interacts with the proline-rich region of Shank proteins [38,39] (Fig. 1).

Shank proteins are encoded by three genes, *Shank1/ProSAP3*, *Shank2/ProSAP1*, and *Shank3/ProSAP2*. Mutations in *Shank3* are strongly associated with neuropsychiatric symptoms (such as developmental delay and severely delayed or absent speech) [42] in individuals with 22q13 deletion syndrome (also called Phelan-McDermid syndrome) [43]. Several *de novo* mutations in *Shank3* have been identified in patients with ASD [6, 22–24, 30]. In addition, several *de novo* deletions and mutations in *Shank2* [5,44,45] and *Shank1* [10,32] were identified in individuals with ASD. A meta-analysis of Shank mutations in 5,657 patients with ASD identified that 0.04%, 0.17%, and 0.69% of patients with ASD had mutations in *Shank1*, *Shank2*, and *Shank3* genes, respectively [30].

2.2. Comparisons of the behavioral phenotypes of Shank mutant mice to the symptoms of patients with ASD

Although mouse behavior cannot be equated with human behavior, researchers investigate mouse behavior to understand human behavior. Mouse behavior can be utilized to study various functions of specific brain regions and circuits associated with particular behavior [46–48]. Researchers have generated many *Shank* mutant mice with genetic mutations found in individuals with ASD and have established

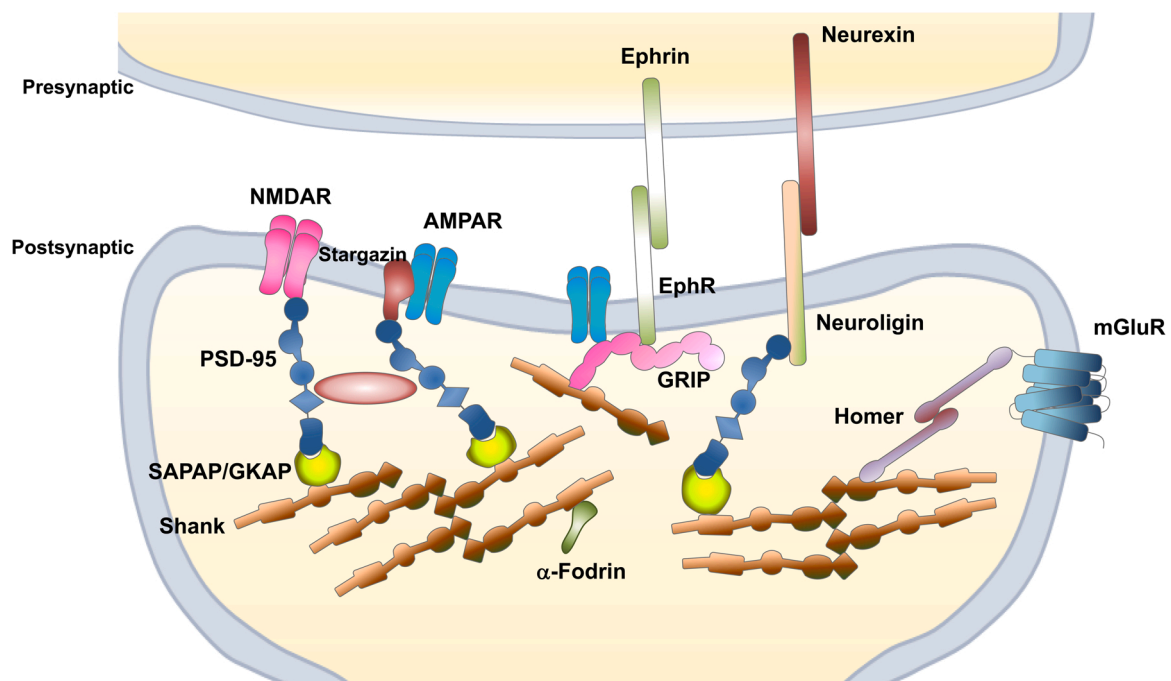


Fig. 1. Postsynaptic scaffolding protein networks at the postsynaptic density (PSD) of the glutamatergic synapse. Trans-synaptic complexes linking the pre- and postsynapse include the ephrin-ephrin receptor and neurexin-neuroligin complexes. Shank proteins directly interact with α -fodrin, SAPAP/GKAP, and Homer. Two major ionotropic glutamate receptors, including the AMPA receptor (AMPA) and NMDA receptor (NMDAR), and metabotropic glutamate receptors (mGluRs) indirectly interact with Shank. PSD-95 interacts with SAPAP/GKAP, neuroligin, and stargazin. Shank proteins are multimerized through their SAM domain. NMDA, *N*-methyl-D-aspartate; AMPA, α -amino-3-hydroxy-5-methyl-4-isoxazolepropionic acid; SAPAP, SAP90/PSD-95-associated protein; GKAP, guanylate kinase-associated protein; SAM, the sterile alpha motif.

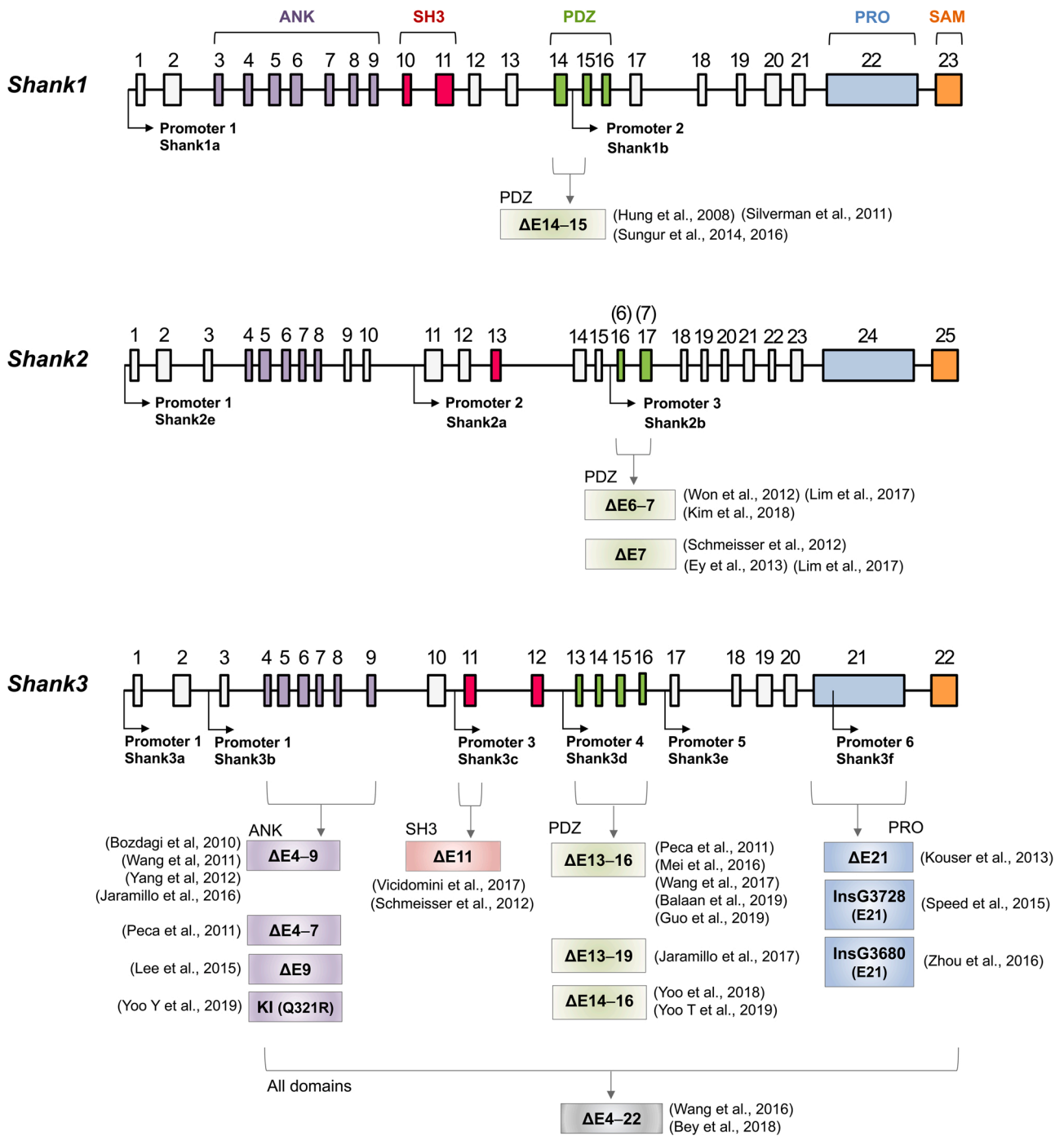


Fig. 2. Shank postsynaptic scaffolding protein gene mutations in mice causing autism spectrum disorder-related phenotypes. Schematic diagrams of the structure of mouse *Shank* genes, including exons (numbered square) and introns, and the domain structure of Shank proteins. The domain names are indicated above the corresponding exons. Arrows indicate promoters. Information on *Shank* mutant mice is shown below the targeted domain or exons. Note that exons 16 and 17 in the full-length *Shank2e* correspond to exons 6 and 7 in *Shank2a*. ANK, ankyrin repeat domain; SH3, Src homology 3 domain; PDZ, PSD-95/Discs large/Zona occludens-1 domain; PRO, proline-rich region; SAM, sterile alpha motif domain; KI, Knock-in. Refer to [Tables 1–3](#) for detailed phenotypical information on studies using *Shank* mutant mice.

appropriate behavioral tests that can be applied to study and compare the symptoms examined in patients with ASD [48,49].

Individuals with ASD exhibit impaired social interactions with other people; they often feel more comfortable with objects than with people. These behavioral traits can be assessed in mice using animal behavioral tests, such as the three-chamber sociability test, which evaluates the social preference/interaction and social novelty recognition of novel mice over novel objects. In addition, individuals with ASD exhibit repetitive behaviors, such as rocking and hand-flapping. These behavioral

traits can be assessed by examining self-grooming, marble burying, and digging behaviors in *Shank* mouse models. Abnormal social communication, having difficulties in understanding others' emotions, and non-verbal social skills, such as eye contact, facial expression, and body language, are also clinical diagnostic features of ASD. These behaviors can be evaluated using ultrasonic vocalizations (USVs) in *Shank* mouse models. Mice emit USVs in response to maternal separation in neonates, intruders to communicate anxiety or fear, and male-female courtship interactions in adults [48,50].

In addition to the core symptoms of ASD described above, increased anxiety is often present in patients with ASD. Anxiety is observed in most neuropsychiatric disorders and is usually associated with, and thus difficult to isolate from, decreased social interaction and repetitive behavior [48]. Anxiety levels in *Shank* mouse models are measured using the open-field test, elevated plus or zero maze, and light-dark test. Mice with high levels of anxiety usually show less time spent in the center of the arena in the open field, less time exploring the open arms in the elevated plus or zero mazes, and increased latency to the brightly lit area in the light-dark test. Most patients with ASD have mild to moderate defects in intellectual ability, while some have average to above-average intellectual ability. Intellectual ability is mostly assessed by performing the original learning of the Morris water maze (MWM) task with *Shank* mouse models [48,49]. Cognitive flexibility deficit is also a feature of patients with ASD [51,52]. Cognitive flexibility is usually evaluated in *Shank* mouse models using the reversal learning of the MWM task. A behavioral phenotype does not solely match a specific ability. Instead, behavior results from a very complicated network among several functions, which should be considered when interpreting behavioral phenotypes obtained from mouse models.

2.3. *Shank1* mutant mice associated with ASD

Mutations in *Shank1* have been found in patients with ASD [10,32]. Thus far, only a single *Shank1* mutant mouse model of ASD has been generated by deleting exons 14 and 15, which encode the PDZ domain, resulting in the complete elimination of all *Shank1* protein isoforms [53]. Using the *Shank1*^{ΔE14–15} mutant line, ASD-related behavioral tests assessing the severity of social interaction, novelty, and communication, repetitive behavior, anxiety, learning and memory, cognitive flexibility, and synaptic defects in biochemistry, structure, and function were evaluated (Table 1). In this *Shank1*^{ΔE14–15} mutant mouse line [53], increased self-grooming in adult *Shank1*^{+/-} heterozygous mice in the social context, but not in juvenile mice, was examined [54]. In addition, isolation-induced USVs were reduced in isolated pups, and an inverted U-shaped developmental USV emission pattern in terms of developmental peak was delayed from P6 to P9 [55]. Enhanced anxiety-like behaviors were observed with less time spent in the center zone in the open field arena and increased latency to the light side in the light-dark test in 3–5-month-old *Shank1*^{ΔE14–15} mutant mice [53]. However, unaltered anxiety-like behavior in the elevated plus maze and mild anxiety-like behavior in the light-dark test were examined in 5–6- and 6–7-week-old, respectively, *Shank1*^{ΔE14–15} mutant mice where several behavioral experiments were sequentially performed [26]. Interestingly, spatial original and reversal learnings in the eight-arm radial maze task were improved, but long-term memory retention in the same task was impaired in *Shank1*^{ΔE14–15} mutant mice [53]. Furthermore, contextual fear memory was impaired in *Shank1*^{ΔE14–15} mutant mice [53].

The expression levels of PSD proteins, such as SAPAP/GKAP and Homer, were biochemically decreased in the adult forebrain tissues of *Shank1*^{ΔE14–15} mutant mice [53]. In addition, reduced SAPAP/GKAP but unaffected Homer expression levels were detected immunocytochemically in cultured hippocampal neurons from *Shank1*^{ΔE14–15} mutant mice [53]. The input-output curve shifted downward at the Schaffer collateral-CA1 synapse in *Shank1*^{ΔE14–15} mutant mice, indicating a reduction in basal synaptic transmission. This reduction was not due to a change in presynaptic release probability because unchanged paired-pulse facilitation was observed [53]. Although spatial original and reversal learnings were improved in *Shank1*^{ΔE14–15} mutant mice, long-term potentiation (LTP) and long-term depression (LTD) were normal in these mice [53].

2.4. *Shank2* mutant mice associated with ASD

Two lines of *Shank2* mutant mice that lack all *Shank2* isoforms by the deletion of the PDZ domain-coding exons 6–7 (*Shank2*^{ΔE6–7}) [56–58] or

exon 7 (*Shank2*^{ΔE7}) [57,59,60] have been reported by two groups [58, 60] (Fig. 2). These two lines of *Shank2* knockout (KO) mice exhibited shared and distinct physiological and behavioral phenotypes (Table 2). Reduced social preference (mouse over the object) and normal social novelty recognition (novel mouse over a familiar one) in the three-chamber test were examined in *Shank2*^{ΔE6–7} mutant mice [58], whereas reduced social novelty in the three-chamber test and delayed first contact in male mice with estrus female mice were examined in *Shank2*^{ΔE7} mutant mice [60]. *Shank2*^{ΔE7} mutant mice displayed excessive self-grooming in females but not in males [60]. *Shank2*^{ΔE6–7} mutant mice showed enhanced repetitive jumping behaviors and normal grooming in the home cage but increased grooming in a new environment, such as a novel object recognition arena [58]. Both mutant lines showed reduced digging repetitive behavior and reduced call rates with a delayed first call [58–60]. Increased levels of anxiety in the elevated plus maze test in *Shank2*^{ΔE6–7} mutant mice [58] and during the light-dark box test in *Shank2*^{ΔE7} mutant mice [60] were examined. Spatial learning and memory in the MWM task were impaired in both *Shank2* mutant lines [58,60].

In a recent follow-up study [56], conditional mutant *Shank2* mice with *Shank2* deletion in excitatory or inhibitory neurons were generated to investigate which cell types contributed to the phenotypes observed in the global KO of *Shank2*^{ΔE6–7} mice [58]. The social phenotypes of reduced social approach but normal social novelty recognition in the three-chamber test, which were observed in the global KO of *Shank2*^{ΔE6–7} mice [58], were also mimicked in the conditional KO of *Shank2* in excitatory neurons [56], indicating that excitatory neurons in the brain could mainly contribute to such social behaviors. Mice with conditional KO of *Shank2* in excitatory neurons and global KO of *Shank2*^{ΔE6–7} also showed similar repetitive behaviors, such as normal self-grooming and reduced digging [56,58]. USV phenotypes, such as less frequent calls and delayed first calls, which were observed in mice with global KO of *Shank2*^{ΔE6–7} [58], were similarly examined in mice with conditional KO of *Shank2* in the inhibitory neurons [56]. Another study reported that restoring GABAergic synaptic transmission following treatment with L838,417, an α2-, α3-, and α5-specific γ-aminobutyric acid type A (GABA_A) receptor positive allosteric modulator, reversed spatial memory deficits but not social deficits in *Shank2*^{ΔE6–7} KO mice [57].

Regarding synapse structure and function, no alterations in PSD length and thickness were found in either line of *Shank2* mutant, while no changes in PSD density in *Shank2*^{ΔE6–7} and spine density in *Shank2*^{ΔE7} mutant mice were observed [58,60]. In the hippocampus of *Shank2*^{ΔE6–7} mutant mice, the miniature excitatory postsynaptic current (mEPSC) amplitude and frequency were unaffected. On the other hand, LTP induced by high-frequency or theta burst stimulation and LTD induced by low-frequency stimulation, but not by mGluR activation, were impaired [58]. However, *Shank2*^{ΔE7} mutant mice showed a reduced frequency but an unaltered amplitude of mEPSCs, enhanced LTP, and unaltered LTD in the hippocampus [60]. GABA synaptic transmission was impaired in CA1 neurons in *Shank2*^{ΔE6–7} but not in *Shank2*^{ΔE7} mutant mice [57].

2.5. *Shank3* mutant mice associated with ASD

Shank3 has six isoforms that exhibit differential expression patterns across brain regions, developmental stages, and cell types [61] (Fig. 2). To investigate the function and mechanisms of *Shank3* in ASD, various *Shank3* KO mouse lines lacking some or all of the *Shank3* isoforms were generated by the deletion of specific exon(s) targeting the functional domains of *Shank3* or by the insertion of a single nucleotide based on the mutation information obtained from individuals with ASD. The first *Shank3* mutant mice lacking the ankyrin repeat domain-coding exons 4–9 (*Shank3*^{ΔE4–9}) were reported by the Buxbaum group [62] (Table 3). Subsequently, a study using the same mouse line as *Shank3*^{ΔE4–9} [63] and two studies using independently generated *Shank3*^{ΔE4–9} mouse lines

Table 1
Behavioral and non-behavioral phenotypes of *Shank1* mutant mice associated with autism spectrum disorder.

Targeted scaffold protein	Mouse model details	Behavioral phenotypes						Non-behavioral phenotypes			References
		Social behaviors	Repetitive behaviors	USVs	Anxiety-like behaviors	Learning and memory	Other behavioral phenotypes	Biochemistry, morphology & structure	Shank expression	Synaptic function	
Shank1	PDZ domain-coding exons 14–15 deletion	N/A	N/A	N/A	<ul style="list-style-type: none"> Spent less time in the center zone Increased latency to the light side in the light-dark test 	<ul style="list-style-type: none"> Improved spatial original and reversal learning but impaired long-term retention in the eight-arm radial maze task Impaired contextual fear memory 	<ul style="list-style-type: none"> Normal in home cage but less active in a novel open-field Mild deficit in motor performance in rotarod 	<ul style="list-style-type: none"> Reduced spine length and width Thinner PSDs Slightly reduced spine density Reduced GKAP and Homer in adult forebrain (Western blot) Reduced GKAP but unaffected Homer in cultured hippocampal neurons (ICC) 	<ul style="list-style-type: none"> Almost loss of Shank1 proteins in the forebrain membrane fraction Complete loss of Shank1 proteins in PSD fractions No compensatory increases of Shank1 and Shank3 proteins (detected by pan-Shank antibody) 	<ul style="list-style-type: none"> Reduced input-output at SC-CA1 synapse Unchanged PPF and NMDA/AMPA ratio Unaltered mEPSC amplitude but reduced mEPSC frequency Unaltered LTP and LTD 	Hung et al., 2008
		<ul style="list-style-type: none"> Normal juvenile reciprocal social interaction, including nose-to-nose sniff, anogenital sniff, body sniff, push and crawl, pushing past, and follow Lack of sociability in the three-chamber test 	<ul style="list-style-type: none"> Unaltered self-grooming at age of 10–12 weeks 	N/A	<ul style="list-style-type: none"> Mild anxiety-like behavior in the light-dark test Unaltered in the elevated plus maze 	N/A	<ul style="list-style-type: none"> No deficits in non-social and social olfactory capabilities Reduced exploratory locomotion in a novel open-field Reduced motor coordination, balance and neuromuscular strength in rotarod and inverted wire hang tests Unaltered in the acoustic startle response and in PPI of acoustic startle at any prepulse level Normal pain sensitivity 	N/A	N/A	N/A	Silverman et al., 2011
		N/A	<ul style="list-style-type: none"> Unaltered self-grooming and digging in juveniles Increased self-grooming but normal digging in the social context in adults 	N/A	N/A	N/A	<ul style="list-style-type: none"> Reduced locomotor activity (such as line crossings and rearing) in juveniles Reduced rearing in the social context in adults 	N/A	N/A	N/A	Sungur et al., 2014

(continued on next page)

Table 1 (continued)

Targeted scaffold protein	Mouse model details	Behavioral phenotypes						Non-behavioral phenotypes			References
		Social behaviors	Repetitive behaviors	USVs	Anxiety-like behaviors	Learning and memory	Other behavioral phenotypes	Biochemistry, morphology & structure	Shank expression	Synaptic function	
		N/A	<ul style="list-style-type: none"> Unaltered marble burying irrespective of social context in adults 	<ul style="list-style-type: none"> Reduced number of USV Reduced call peak amplitude but unaltered call duration and peak frequency in isolated pups Delayed from P6 to P9 in inverted U-shaped developmental USV emission pattern 	N/A	N/A	N/A	N/A	N/A	N/A	Sungur et al., 2016

Abbreviations: AMPA, L- α -amino-3-hydroxy-5-methyl-4-isoxazolepropionate; GKAP, guanylate kinase-associated protein; ICC, immunocytochemistry; LTD, long-term depression; LTP, long-term potentiation; mEPSC, miniature excitatory postsynaptic current; NMDA, N-methyl-D-aspartate; N/A, not applicable as the experiment was not conducted; PDZ, PSD-95/Discs large/Zona occludens-1 domain; PPF, paired-pulse facilitation; PPI, prepulse inhibition; PSD, postsynaptic density; SC-CA1, Schaffer collateral-Cornu Ammonis 1; Shank, SRC homology 3 (SH3) and multiple ankyrin repeat domain; USVs; ultrasonic vocalizations.

Table 2
Behavioral and non-behavioral phenotypes of *Shank2* mutant mice associated with autism spectrum disorder.

Targeted scaffold protein	Mouse model details	Behavioral phenotypes						Non-behavioral phenotypes			References
		Social behaviors	Repetitive behaviors	USVs	Anxiety-like behaviors	Learning and memory	Other behavioral phenotypes	Biochemistry, morphology & structure	Shank expression	Synaptic function	
Shank2	PDZ domain-coding exons 6–7 deletion and a frame shift	<ul style="list-style-type: none"> Reduced preference to mouse over object in the three-chamber Normal preference to novel mouse over a familiar one in the three-chamber 	<ul style="list-style-type: none"> Enhanced repetitive jumping Normal grooming in home-cage but increased grooming in NOR arena Decreased digging 	<ul style="list-style-type: none"> Less frequent calls and delayed the first call (males toward novel females) 	<ul style="list-style-type: none"> Increased in an elevated plus maze 	<ul style="list-style-type: none"> Impaired spatial learning and memory in MWM test Normal in NOR 	<ul style="list-style-type: none"> Normal olfactory function Less efficient pup retrieval of female mice Impaired nesting behavior Hyperactivity in open-field 	<ul style="list-style-type: none"> No alterations in PSD density, length, and thickness 	<ul style="list-style-type: none"> Undetectable Shank2 mRNA and Shank2 proteins in the brain No compensatory increases in Shank1 and 3 proteins 	<ul style="list-style-type: none"> Unaltered input-output curve, PPR, and mEPSC amplitude and frequency in the hippocampus Reduced NMDA/AMPA ratio Impaired LTP (HFS, theta-burst) Abolished LFS-LTD but normal mGluR-LTD Unaltered NMDA/AMPA ratio in mPFC 	Won et al., 2012
		<ul style="list-style-type: none"> Social interaction deficit in the three-chamber 	N/A	N/A	<ul style="list-style-type: none"> Normal anxiety level in the elevated zero maze, but decreased time spent in the center in the open-field 	<ul style="list-style-type: none"> Impaired spatial learning and memory in MWM test 	<ul style="list-style-type: none"> Hyperactive in the elevated zero maze and open-field 	<ul style="list-style-type: none"> Reduced GABA_A receptor $\alpha 2$ subunit 	N/A	<ul style="list-style-type: none"> Impaired GABA synaptic transmission and thus reduced I/E ratio in CA1 neurons Unaltered PPR 	Lim et al., 2017
		PDZ domain-coding exons 6–7 deletion in inhibitory neuron (Viaat-Cre;Shank2 ^{fl/fl})	<ul style="list-style-type: none"> Normal social approach and social novelty recognition in the three-chamber (9–12 weeks old mice) Reduced male-female social interaction 	<ul style="list-style-type: none"> Enhanced self-grooming but normal digging and jumping (10–13 weeks old mice) in home cages Enhanced head bobbing (11–13 weeks old mice) in the hole-board test 	<ul style="list-style-type: none"> Reduced number of calls and increased latency to the first call (10–13 weeks old mice) 	<ul style="list-style-type: none"> Normal anxiety-like behaviors in open-field, the elevated plus maze (11–14 weeks old mice), and the light-dark test 	N/A	<ul style="list-style-type: none"> Hyperactivity in open-field (a novel environment) but normal locomotor activity in the Laboras test (a familiar environment) 	<ul style="list-style-type: none"> Marked reductions of Shank2 in the striatum and cerebellum but not in the cortex and hippocampus (10 weeks old) Unchanged expressions of Shank1 and Shank3 proteins in the cortex, hippocampus, striatum, and cerebellum 	<ul style="list-style-type: none"> (In the dorsolateral striatum) Normal mEPSC amplitude and frequency Reduced mIPSC amplitude and frequency Reduced frequency but unaltered amplitude of sEPSC Normal frequency but reduced amplitude of sIPSC (In the hippocampus) Normal mEPSC and mIPSC amplitude and frequency (In the hippocampus) 	Kim et al., 2018
	PDZ domain-coding exons 6–7 deletion in excitatory neuron (CaMKII-Cre; Shank2 ^{fl/fl})	<ul style="list-style-type: none"> Reduced social approach, but normal social novelty recognition in the three-chamber (9–12 weeks old; males) 	<ul style="list-style-type: none"> Normal self-grooming and jumping Reduced digging Normal head bobbing in the hole-board test 	<ul style="list-style-type: none"> Normal numbers of calls, but increased latency to the first call (9–12 weeks old mice) 	<ul style="list-style-type: none"> Increased anxiety-like behavior in the center region of the open-field Normal anxiety-like behavior (12–15 weeks old) 	N/A	<ul style="list-style-type: none"> Mild hyperactivity in open-field (a novel environment) and in the Laboras test (a familiar environment) 	<ul style="list-style-type: none"> Strong reductions of Shank2 in the cortex and hippocampus but no changes in the striatum and cerebellum (12 weeks old) Unchanged expressions of Shank1 and Shank3 	<ul style="list-style-type: none"> Reduced frequency but unaltered amplitude of mEPSC Unaltered mIPSC amplitude and frequency 		

(continued on next page)

Table 2 (continued)

Targeted scaffold protein	Mouse model details	Behavioral phenotypes						Non-behavioral phenotypes			References
		Social behaviors	Repetitive behaviors	USVs	Anxiety-like behaviors	Learning and memory	Other behavioral phenotypes	Biochemistry, morphology & structure	Shank expression	Synaptic function	
		<ul style="list-style-type: none"> Reduced male-female social interaction 			<ul style="list-style-type: none"> Increased in the elevated plus maze Increased in the light-dark test 				<ul style="list-style-type: none"> proteins in the cortex, hippocampus, striatum, and cerebellum 	<ul style="list-style-type: none"> Normal PPF 	
	PDZ domain-coding exon 7 deletion	N/A	N/A	N/A	N/A	<ul style="list-style-type: none"> Impaired spatial learning and memory in MWM test 	N/A	<ul style="list-style-type: none"> No change in GABA_A receptor $\alpha 2$ subunit 	N/A	<ul style="list-style-type: none"> No change in GABA synaptic transmission and thus I/E ratio in CA1 neurons 	Lim et al., 2017
		N/A	N/A	<ul style="list-style-type: none"> Lower call rate with a different call distribution in males and females Reduced call duration in adult female mice 	N/A	N/A	N/A	N/A	N/A	N/A	Ey et al., 2013
		<ul style="list-style-type: none"> Delayed first contact in male mice with estrus female mice Reduced social novelty in the three-chamber 	<ul style="list-style-type: none"> Extended self-grooming in females but not in male mice Shorter digging 	<ul style="list-style-type: none"> Higher call rate in female pups Longer latency to first call and lower call rate in female adults 	<ul style="list-style-type: none"> Increased anxiety-like behavior in the light-dark box test 	<ul style="list-style-type: none"> Normal working memory in Y-maze and NOR 	<ul style="list-style-type: none"> Normal motor coordination in rotarod Enhanced locomotor activity in open-field Normal olfaction in home-cage odor preference test 	<ul style="list-style-type: none"> Reduced spine density No alteration of PSD length or thickness Enhanced GluN1 and Shank3 in whole brain 	<ul style="list-style-type: none"> Unaltered Shank3 mRNA level in the whole brain Complete loss of all isoforms of Shank2 protein in the whole brain, hippocampus, and cerebellum homogenates Normal Shank3 but significant reduced Shank1 expression in crude synaptosome fraction of hippocampus at P25 and P70 Normal Shank3 and Shank1 expression in crude synaptosome fraction of striatum at P25, but significant increase of Shank3 expression in crude synaptosome fraction of striatum at P70 	<ul style="list-style-type: none"> No changes in the excitability of presynaptic fibers, the intrinsic firing threshold, and the whole-cell input resistance of CA1 pyramidal cells Reduced basal hippocampal synaptic transmission Reduced mEPSC frequency and unaltered amplitude in the hippocampus Enhanced NMDA-mediated currents Increased NMDA/AMPA ratio Enhanced hippocampal HFS-LTP and unaltered LTD induced by paired pulse 	Schmeisser et al., 2012

Abbreviations: AMPA, L- α -amino-3-hydroxy-5-methyl-4-isoxazolepropionate; GABA, gamma-aminobutyric acid; HFS, high-frequency stimulation; I/E, inhibition/excitation; LFS, low-frequency stimulation; LTD, long-term depression; LTP, long-term potentiation; mEPSC, miniature excitatory postsynaptic current; mGluR, metabotropic glutamate receptor; mIPSC, miniature inhibitory postsynaptic current; mPFC, medial prefrontal cortex; MWM, Morris water maze; NMDA, N-methyl-D-aspartate; NOR, novel object recognition; N/A, not applicable as the experiment was not conducted; PDZ, PSD-95/Discs large/Zona occludens-1 domain; PPF, paired-pulse facilitation; PPR, paired-pulse ratio; PSD, postsynaptic density; CA1, Cornu Ammonis 1; sEPSC, spontaneous excitatory postsynaptic current; Shank, SRC homology 3 (SH3) and multiple ankyrin repeat domain; USVs; ultrasonic vocalizations.

[27,64] were reported. In addition, the Feng group reported two different mouse lines of *Shank3* that were generated by deleting the PDZ domain-coding exons 13–16 (*Shank3*^{ΔE13–16}) or by deleting the ankyrin repeat domain-coding exon 4–7 (*Shank3*^{ΔE4–7}) [25]. Moreover, *Shank3* mutant mice were generated by deleting the ankyrin repeat domain-coding exon 9 (*Shank3*^{ΔE9}) [65], SH3 domain-coding exon 11 (*Shank3*^{ΔE11}) [60], or proline-rich domain-coding exon 21 (*Shank3*^{ΔC/ΔC}) [66]. A single guanine nucleotide (G) insertion (InsG) mutant of *Shank3* was generated by inserting an extra G into intron 20 near exon 21 (*Shank3*^{InsG3728}) [67]. Subsequently, the same group (the Powell group) that published the studies of Krouser et al. (2013), Speed et al. (2015), and Jaramillo et al. (2016) generated another *Shank3* mutant mouse (*Shank3*^{ΔE13}) by inserting a neo-stop cassette into between exons 12 and 13 [68]. The Feng group also created a mouse line with an ASD patient-associated G insertion at cDNA position 3680 (*Shank3*^{InsG3680}) [69]. Importantly, the Jiang group that generated *Shank3*^{ΔE4–9} mutant mice [27] utilized a two-step gene targeting and Cre/LoxP strategy and successfully generated *Shank3* complete KO (*Shank3*^{ΔE4–22}) mice [70]. In *Shank3* complete KO (*Shank3*^{ΔE4–22}) mice, exons 4–22, including the coding sequences for all *Shank3* isoforms, were deleted, resulting in the lack of all *Shank3* isoforms. Recently, global and conditional KO mice with deletion of the PDZ domain-coding exons 14–16 of *Shank3* (*Shank3*^{ΔE14–16}) [71,72] and a knock-in (KI) mouse line carrying the human Q321R missense mutation that occurs in the ankyrin repeat region domain of *Shank3* in an individual with ASD were generated [73].

2.5.1. Behavioral phenotypes of *Shank3* mutant mice

Although *Shank3* mutant mice with deletions of the same exon(s) exhibit different behavioral phenotypes, most *Shank3* mutant mice display ASD-associated behavioral phenotypes, including social interaction impairments, repetitive self-grooming, and/or anxiety-like behaviors (Table 3). *Shank3*^{ΔE4–9} [27,63,64], *Shank3*^{ΔE13–16} [25,74,75], *Shank3*^{ΔE11} [76], *Shank3*^{ΔE21} [66], *Shank3*^{InsG3680(E21)} [69], *Shank3*^{Δ14–16} [71], *Shank3*^{Δ14–16} glutamatergic [72] or GABAergic neuronal deficient [71], and complete *Shank3* KO (*Shank3*^{ΔE4–22}) [70] mice displayed increased self-grooming behaviors (from moderately increased to self-injurious). On the other hand, *Shank3*^{ΔE4–7} [25], *Shank3*^{ΔE9} [65], and *Shank3*^{InsG3728} [67] mice showed no alterations in self-grooming.

Most *Shank3* mutant mice displayed impaired social ability and interaction, except *Shank3*^{ΔE9} [65], *Shank3*^{InsG3728} [67], *Shank3*^{ΔE14–16} global KO or GABAergic neuronal deficient [71], *Shank3*^{ΔE14–16} glutamatergic neuronal deficient [72], and KI mice carrying the Q321R mutation [73]. Using the same line of *Shank3*^{ΔE13–16} mutant mice with self-injurious grooming and reduced social interaction [25,75], other ASD-related behavioral tests were further investigated to examine infants (<3 weeks old) and juveniles (3–6 weeks old) [77]. Social interaction phenotypes observed in the three-chamber test were sex-dependent, showing reduced social interaction in male mice but normal interaction in female juvenile *Shank3*^{ΔE13–16} mice. In contrast, increased self-grooming behaviors were showed with no difference between male and female juvenile *Shank3*^{ΔE13–16} mice [77].

No alterations in USVs or anxiety-like behaviors were observed in *Shank3*^{ΔE13–16} mice compared to littermate control mice [77]. In contrast, another group reported that the same line of *Shank3*^{ΔE13–16} mice exhibit high levels of anxiety with decreased rearing activity in the open field test, less time exploring the open arms in the elevated zero maze, and increased latency to enter the brightly lit area in the light-dark emergence test [25]. Altered USVs were examined in *Shank3*^{ΔE4–9} [27, 62–64], *Shank3*^{ΔE4–22} [70,78], and *Shank3*^{ΔE14–16} GABAergic neuronal deficient [71] mice.

Shank3 mutant mice display different learning and memory performance. *Shank3*^{ΔE4–9} mutant mice showed intact [63,64] but also retarded [27] spatial original and reversal learning in the MWM. *Shank3*^{ΔE13–16} mice showed normal spatial learning in MWM [25],

whereas *Shank3*^{ΔE9} [65], *Shank3*^{ΔE13–19} [68], and *Shank3*^{InsG3728} [67] mice showed impaired or mildly retarded spatial learning in MWM tasks. Furthermore, *Shank3*^{ΔE11} [76] and *Shank3*^{ΔE4–22} [70] mice exhibited normal original but impaired reversal spatial learning in MWM tasks, whereas *Shank3*^{ΔE21(ΔC/ΔC)} mice showed impaired original spatial learning but normal reversal learning in MWM tasks [66].

Using conditional KO or expression technology, specific brain regions and/or cell types that contribute to distinct behavioral phenotypes related to ASD have further been identified [71,72,78,79]. Similar to the social interaction deficits observed in global *Shank3*^{ΔE13–16} KO mice [25,75], conditional KO of *Shank3*^{ΔE13–16} in the glutamatergic synapses of pyramidal neurons in the anterior cingulate cortex (ACC) led to social interaction deficits comparable to those following global *Shank3*^{ΔE13–16} KO mice but did not affect grooming, marble burying, novel object preference, and anxiety levels compared to wild-type (WT) control mice [79]. In addition, restoration of *Shank3* proteins in the ACC improved social behavior in *Shank3* mutant mice [79]. Together, these data indicate that the ACC is involved in the *Shank3*-mediated regulation of social interaction function, but not grooming, marble burying, novel object preference, or anxiety. Interestingly, optogenetic activation of ACC pyramidal neurons rescues anxiety-like behavior and social interaction in *Shank3*^{ΔE13–16} KO mice [79], indicating that anxiety-like behavior is regulated by ACC pyramidal neuron activation. In addition, the USV deficits observed in global *Shank3*^{ΔE14–16} mice were attributed to GABAergic neurons but not glutamatergic neurons [71,72]. Furthermore, the loss of *Shank3*^{ΔE4–22} in forebrain excitatory neurons or striatal medium spiny neurons (MSNs) was responsible for behavioral phenotypes of repetitive self-grooming or repetitive exploration, respectively [70,78]. The Feng group also reported that selective enhancement of striatopallidal (indirect pathway) MSN activity using a Gq-coupled human M3 muscarinic receptor, a type of designer receptors exclusively activated by designer drugs (DREADD), reduced repetitive grooming behavior [75]. This finding indicates that the indirect striatal pathway is responsible for the repetitive behavior in *Shank3*^{ΔE13–16} mutant mice. A study using conditional KO of *Shank3* in specific cell types further revealed that instrumental learning is not dependent on *Shank3* in forebrain excitatory or basal ganglia inhibitory neurons [78]. The same study also found that prepulse inhibition and anxiety-like behaviors, which are augmented and reduced, respectively, in global *Shank3*^{ΔE4–22} mice, are due to the loss of *Shank3* in MSNs [78].

2.5.2. Biochemical, structural, and functional phenotypes of synapses in *Shank3* mutant mice

Spine morphology, synapse structural composition, and electrophysiological recordings were also examined to investigate structural and functional characteristic changes in *Shank3* mutant mice. Like the differences observed in the behavioral phenotypes of *Shank3* mutant mice, the structure and function of synapses were also differentially affected in various *Shank3* mutant mice (Table 2). In the hippocampus of *Shank3*^{ΔE4–9} mutant lines, reduced input-output curve, impaired LTP but normal LTD [62,63], reduced amplitudes and increased frequencies of mEPSCs, and defective spine remodeling during LTP [62] were examined. Interestingly, spine density and length [27] and electrophysiological features, including input-output relationship, mEPSCs, and LTP [27,62,63] were differentially affected in an age-dependent manner, suggesting developmental stage-dependent differential regulatory mechanisms underlying ASD. In another line of *Shank3*^{ΔE4–9} mutant mice, Homer1b/c, GluA2, and GluA3 synaptic protein expression decreased in the striatal synaptosomal fraction of *Shank3*^{ΔE4–9} mutant mice [64]. In the same mouse line, the striatum and hippocampus exhibited different electrophysiological features. A significant reduction in NMDA/AMPA ratio, but no changes in mEPSC amplitude and frequency, were observed in the striatum, whereas in the hippocampus, no alterations in baseline synaptic transmission, NMDA/AMPA ratio, mEPSC amplitude and frequency, paired-pulse ratio (PPR), input-output relationship, and mGluR-LTD, but a reduction in LTP were

Table 3

Behavioral and non-behavioral phenotypes of *Shank3* and *Shank1/Shank3* double mutant mice associated with autism spectrum disorder.

Targeted scaffold protein	Mouse model details	Behavioral phenotypes						Non-behavioral phenotypes			References
		Social behaviors	Repetitive behaviors	USVs	Anxiety-like behaviors	Learning and memory	Other behavioral phenotypes	Biochemistry, morphology & structure	Shank expression	Synaptic function	
Shank3	ANK domain-coding exons 4–9 deletion (3 lines)	<ul style="list-style-type: none"> Reduced social sniffing in adult male-female social interaction 	N/A	<ul style="list-style-type: none"> Reduced during the social interaction 	N/A	N/A	<ul style="list-style-type: none"> Normal in olfactory habituation and dishabituation 	<ul style="list-style-type: none"> Defective spine remodeling during LTP 	<ul style="list-style-type: none"> Complete loss of full-length <i>Shank3</i> mRNA Complete loss of full-length Shank3 protein in the PSD fraction 	<ul style="list-style-type: none"> In the hippocampus (3-4 weeks old mice), reduced mEPSC amplitude, reduced input-output curve, impaired LTP but normal LTD Reduced AMPA receptor immunoreactivity 	Bozdagi et al., 2010
		<ul style="list-style-type: none"> Normal in the three-chamber and freely-moving dyads Mildly impaired in juvenile reciprocal social interaction 	<ul style="list-style-type: none"> Elevated self-grooming in males 	<ul style="list-style-type: none"> Mostly normal 	<ul style="list-style-type: none"> Normal in the elevated plus maze and light-dark exploration (no sex differences) 	<ul style="list-style-type: none"> Normal original and reversal learning in MWM Impaired NOR Normal contextual and cued fear conditioning 	<ul style="list-style-type: none"> Impaired rotarod performance Normal PPI of acoustic startle Normal olfaction, sensory gating, and nociception 	N/A	N/A	<ul style="list-style-type: none"> In the hippocampus (4-6 weeks old mice), reduced input-output curve, impaired LTP induction and maintenance, normal LTD 	Yang et al., 2012
		<ul style="list-style-type: none"> Abnormal sociability and interaction 	<ul style="list-style-type: none"> Excessive self-grooming Enhanced repetitive object exploration 	<ul style="list-style-type: none"> More calls in males but fewer calls in females when exposed to unfamiliar mice Less complexed call patterns Altered in duration and frequency 	<ul style="list-style-type: none"> Normal in the light-dark test and the elevated zero maze 	<ul style="list-style-type: none"> Retarded original and reversal learning in MWM 	<ul style="list-style-type: none"> No alteration in olfactory preferences to discriminate urine from saline Abnormal motor performance in open-field and rotarod Normal PPI and startle response 	<ul style="list-style-type: none"> No changes in dendritic branching, spine density, and spine head area in CA1 (P6-7) No changes in PSD length or thickness in CA1 (2-4 months old mice) Reduced spine density but increased length in CA1 (4 weeks old mice) No changes in spine density but reduced length in CA1 (10 weeks old mice) In adult forebrain PSD I fraction, reduced GRAP and Homer1b/c but unaltered Homer1a In adult forebrain SPM fraction, 	<ul style="list-style-type: none"> <i>Shank3a</i> and <i>Shank3b</i> transcripts are absent, but <i>Shank3c</i>, <i>Shank3d</i>, and <i>Shank3e</i> transcripts are present Complete loss of Shank3a protein (~190 kD), but two Shank3 isoforms (~140 kD and ~170 kD proteins) are present 	<ul style="list-style-type: none"> [In the hippocampus (2-4 months old mice)] No alterations in input-output relationship, PPR, mEPSC amplitude and frequency, and mIPSC amplitude and frequency Reduced LTP Inhibited chemical LTP in AMPA receptor distribution 	Wang et al., 2011

(continued on next page)

Table 3 (continued)

Targeted scaffold protein	Mouse model details	Behavioral phenotypes						Non-behavioral phenotypes			References
		Social behaviors	Repetitive behaviors	USVs	Anxiety-like behaviors	Learning and memory	Other behavioral phenotypes	Biochemistry, morphology & structure	Shank expression	Synaptic function	
		<ul style="list-style-type: none"> Abnormal social interaction 	<ul style="list-style-type: none"> Increased self-grooming Normal marble burying 	<ul style="list-style-type: none"> Increased call number at P4 and P6 following separation from mother early in life 	<ul style="list-style-type: none"> Normal in open-field, the dark-light test, and the elevated plus maze 	<ul style="list-style-type: none"> Deficits in spatial novelty recognition and NOR Mostly normal in MWM original and reversal learning except showing an increase in % thigmotaxis during the original learning 	<ul style="list-style-type: none"> Normal nest building Normal locomotor activity in the locomotor box and rotarod Normal in startle, PPI, and fear conditioning 	<ul style="list-style-type: none"> reduced GluA1 and GluN2A but unaltered GluA2 and GluN2B Synaptic proteins expression not altered in striatal lysates but altered in striatal synaptosomes Decreased Homer1b/c, GluA2, and GluA3 expression in the striatal synaptosome fraction 	<ul style="list-style-type: none"> Loss of the two highest molecular weighted Shank3 isoforms, and reduced expression of the 3rd and 7th highest molecular weighted Shank3 isoforms in striatal lysates Loss of the two largest Shank3 isoforms, and reduced expression of other Shank3 isoforms in striatal synaptosome Complete loss of Shank3α protein but unaffected Shank3β and Shank3γ isoforms 	<ul style="list-style-type: none"> (In the hippocampus) No alterations in baseline synaptic transmission, NMDA/AMPA ratio, mEPSC amplitude and frequency, PPR, and input-output relationship Normal mGluR-LTD but reduced hippocampal LTP (In the striatum) A significant reduction in NMDA/AMPA ratio but no changes in mEPSC amplitude and frequency Slight reduction in cortico-striatal synaptic transmission 	<ul style="list-style-type: none"> Jaramillo et al., 2016
	ANK domain-coding exons 4–7 deletion (<i>Shank3A</i> ^{-/-})	<ul style="list-style-type: none"> Normal initiation of social interaction, but perturbed social novelty recognition 	<ul style="list-style-type: none"> Normal grooming 	N/A	<ul style="list-style-type: none"> Normal rearing activity in open-field Similar time spent in the open arms in the elevated zero maze 	N/A	N/A	N/A	<ul style="list-style-type: none"> Complete loss of Shank3α protein (~240 kD), but unaffected Shank3c/d (~190 kD) and Shank3e (~140 kD) isoforms 	<ul style="list-style-type: none"> Altered E/I balance Normal mEPSC but decreased mIPSC frequency in the hippocampus Decreased mIPSC frequency but normal mEPSC in mPFC Normal hippocampal LTP 	<ul style="list-style-type: none"> Peca et al., 2011
	ANK domain-coding exon 9 deletion	<ul style="list-style-type: none"> Normal social interaction and social novelty recognition 	<ul style="list-style-type: none"> Normal grooming but increased rearing in novel environment 	<ul style="list-style-type: none"> Normal in pups 	<ul style="list-style-type: none"> Normal time spent in the center region of the open field arena 	<ul style="list-style-type: none"> Mildly impaired spatial memory in MWM 	<ul style="list-style-type: none"> Normal locomotor activity in open-field 	N/A	<ul style="list-style-type: none"> Complete loss of Shank3α protein (~240 kD), but unaffected Shank3c/d (~190 kD) and Shank3e (~140 kD) isoforms 	<ul style="list-style-type: none"> Altered E/I balance Normal mEPSC but decreased mIPSC frequency in the hippocampus Decreased mIPSC frequency but normal mEPSC in mPFC Normal hippocampal LTP 	<ul style="list-style-type: none"> Lee et al., 2015
	Knock-in mouse carrying the Q321R mutation in the ANK domain	<ul style="list-style-type: none"> Normal social interaction in the three-chamber in heterozygous and 	<ul style="list-style-type: none"> Enhanced self-grooming in home cages with bedding but normal self-grooming in 	<ul style="list-style-type: none"> In heterozygous mutant mice, normal number of calls but increased 	<ul style="list-style-type: none"> In heterozygous mutant male mice, normal in open-field and elevated plus 	<ul style="list-style-type: none"> In homozygous mutant mice, normal NOR (2–4 months old; males) and 	<ul style="list-style-type: none"> Normal locomotor activity in Laboras cages and in open-field in heterozygous 	N/A	<ul style="list-style-type: none"> Significant decrease in Shank3α protein (~240 kD), but no significant changes in 	<ul style="list-style-type: none"> Abnormal EEG patterns in frontal and parietal lobes in homozygous mutant (3 months old; males) 	<ul style="list-style-type: none"> Yoo Y et al., 2019

(continued on next page)

Table 3 (continued)

Targeted scaffold protein	Mouse model details	Behavioral phenotypes						Non-behavioral phenotypes			References
		Social behaviors	Repetitive behaviors	USVs	Anxiety-like behaviors	Learning and memory	Other behavioral phenotypes	Biochemistry, morphology & structure	Shank expression	Synaptic function	
		homozygous mutant mice	Laboras cages in heterozygous and homozygous mutant mice (2–3 and 2 months old, respectively; males) • Suppressed digging in home cages with bedding in heterozygous and homozygous mutant mice (2–3 and 2 months old, respectively; males) • In homozygous mutant female mice, normal self-grooming and digging in home cages with bedding	duration of each calls (2–3 months old; males) when encountered with a novel female stranger • In homozygous mutant mice, normal number and duration of calls (4 months old; males) when encountered with a novel female stranger	maze but anxiolytic in the light-dark test by spending more time in the light chamber • In homozygous mutant male mice, normal in open-field but anxiolytic in the elevated plus maze and light-dark test • In homozygous mutant female mice, normal in the elevated plus maze and light-dark test	contextual fear memory (3–6 months old; males)	and homozygous mutant mice • Suppressed seizure susceptibility in homozygous mutant mice (3–4 months old; males) • Normal somatosensory function in the hot plate (6 months old; males) and von Frey (2 months old; males) tests in homozygous mutant mice	Shank3c/d and Shank3e isoforms in homozygous mutant brains	• Normal mEPSC and mIPSC frequency and amplitude in CA1 pyramidal neurons in homozygous mutant mice (P21–25) • Suppressed neuronal excitability in CA1 pyramidal neurons in homozygous mutant mice (P22–26) • Normal mEPSC and mIPSC frequency and amplitude in dorsolateral striatal neurons in homozygous mutant mice (P28–43)		
	SH3 domain-coding exon 11 deletion	NA	NA	NA	NA	NA	NA	• No changes in CA1 PSD thickness and length • No alteration in CA1 spine density • Reduced AMPA receptors • Increased Shank2 in the Striatum • Increased GluN2B in the hippocampus	• Significantly reduced Shank3 and normal Shank1 and Shank2 expression in crude synaptosome fraction of hippocampus at P70 • Significantly reduced Shank3, significantly increased Shank2, and normal Shank1 expression in crude synaptosome fraction of striatum at P70	NA	Schmeisser et al., 2012
		• Impaired social	• Increased self-grooming	NA	• Normal in the elevated plus maze	• Normal spatial memory in a	• Lower nest building score • Minor deficits	• In PSD fraction, a reduction in Homer1b/c protein	• Complete loss of Shank3 in cultured cortical	• Normal basal membrane properties in	Vicidomini et al., 2017

(continued on next page)

Table 3 (continued)

Targeted scaffold protein	Mouse model details	Behavioral phenotypes						Non-behavioral phenotypes			References
		Social behaviors	Repetitive behaviors	USVs	Anxiety-like behaviors	Learning and memory	Other behavioral phenotypes	Biochemistry, morphology & structure	Shank expression	Synaptic function	
		interaction and recognition	• Fewer marbles buried		• Restricted interest and an avoidance phenotype • Fewer marbles buried	spatial object recognition test • Normal original learning but impaired reversal learning in MWM • Impaired in the reversal phase of T-maze task	in motor coordination (deficits in the pole and rotarod tests but normal in the beam walking test) • Increased aggressive behavior • Hyposensitive to pain in hot-plate test	in the striatum, a reduction in both mGlu5 and Homer1b/c in the cortex, and no changes in mGlu5 and Homer1b/c levels in the hippocampus • Reduced mGlu5/Homer interactions in the striatum and cortex	neurons obtained from <i>Shank3</i> mutant mice	striatal MSNs • Impaired mGlu5-mediated enhancement of NMDA-induced responses	
	PDZ domain-coding exons 13–16 deletion (<i>Shank3B</i> ^{-/-})	• Reduced social interaction and abnormal social novelty recognition • Deficits in dyadic interaction	• Excessive and self-injurious grooming	N/A	• High levels of anxiety showing decreased rearing activity in open-field, less time exploring the open arms in the elevated zero maze, and increased latency to the brightly lit area in light-dark test	• Normal in MWM original and reversal learning (4-5 weeks old males)	• Normal motor learning in the rotarod test	• Altered PSD composition in the striatum • No changes in spine length and head diameter but increased spine neck width in striatal MSNs • Increased striatal volume • Increased dendritic complexity and total length and surface area in the striatal MSNs • Decreased spine density and PSD thickness and length in MSNs	• Complete loss of both Shank3 α and Shank3 β proteins, but reduced expression of Shank3 γ isoform	• Normal presynaptic function in the striatum and hippocampus • Normal NMDA/AMPA ratio in MSNs • Reduced mEPSC amplitude and frequency in MSNs but not altered in the hippocampus	Peca et al., 2011
		N/A	• Increased repetitive self-grooming	N/A	N/A	N/A	• Reduced locomotor activity in the open-field	• Reduced dendritic length and spine density in D2 MSNs	N/A	• Reduced mEPSC frequency and PPR • Impaired LTD specifically in D2 but not in D1 MSNs • No alteration in GABA-mIPSCs in D1 and D2 MSNs • Increased intrinsic excitability in D2 MSNs • Impaired Cav1.3 function in D2 but not in D1 MSNs	Wang et al., 2017
		• Impaired social interaction in	• Increased self-grooming in	• Normal in infant males and females	• Normal in juvenile males and females with	N/A	N/A	N/A	N/A	N/A	Balaan et al., 2019

(continued on next page)

Table 3 (continued)

Targeted scaffold protein	Mouse model details	Behavioral phenotypes					Non-behavioral phenotypes			References	
		Social behaviors	Repetitive behaviors	USVs	Anxiety-like behaviors	Learning and memory	Other behavioral phenotypes	Biochemistry, morphology & structure	Shank expression		Synaptic function
		juvenile males in the three-chamber	juvenile males and females	NA	the elevated plus maze and elevated zero maze	NA		• Reduced dendritic complexity and spine density in the ACC pyramidal neurons • Reduced AMPA receptor-mediated EPSC amplitude and AMPA/NMDA ratio in ACC pyramidal neurons	N/A	• Decreased mEPSC amplitude and frequency in ACC pyramidal neurons • Blocked LTP in ACC pyramidal neurons • No change in PPR • Reduced excitatory synaptic input level in ACC pyramidal neurons	Guo et al., 2019
	Conditional Shank3 deletion in the ACC (used virus injection into WT mice)	• Defects in social interaction behavior • Normal preference in novel object	• Normal grooming • Normal marble burying	NA	• Normal anxiety level in elevated plus maze and open-field	NA		• Reduced expression of GluA1 and GluA2 but higher expression of NR2B	• Almost eliminated major isoforms of Shank3, including α , β , and γ , in the ACC but not in the adjacent motor cortex	• Reductions in mEPSC amplitude and frequency, input-output responses, and AMPA/NMDA ratio • No change in PPR	
	Shank3 fx/fx (exons 13-16)	• No preference for stranger mouse compared with the novel object	• Self-injurious grooming	N/A	• High levels of anxiety showing reduced time in open arm in the elevated zero maze	N/A	• Deficits in exploration in the open-field • Impaired motor coordination in rotarod test	• Reduced PSD proteins (SAPAP3, Homer, NR2A, NR2B, and GluA2) in the striatum • Decreased spine density in MSNs	• Deletion of most major isoforms of Shank3, including α , β , and γ , in striatal PSD	• Decreased pop spike amplitude in the dorsal striatum • Unaltered presynaptic function in the dorsal striatum • Normal mEPSC amplitude but decreased mEPSC frequency in the striatum	Mei et al., 2016
	a transcriptional stop cassette inserted upstream of the PDZ domain-	• Impaired social interaction	• Increased self-grooming • Decreased marble-burying	N/A	• Normal in the open-field and dark-light test • Decrease time spent in the open	• Impaired spatial learning in MWM	• Reduced rearing • No changes in acoustic startle response to	• In striatal synaptosome preparation, decreases in GluA2, GluA3, GluN2A,	• Absence of the three largest Shank3 isoforms but the presence	• Impaired LTP but normal mGluR-LTD in the hippocampus • Intact input-output relationship	Jaramillo et al., 2017

(continued on next page)

Table 3 (continued)

Targeted scaffold protein	Mouse model details	Behavioral phenotypes						Non-behavioral phenotypes			References
		Social behaviors	Repetitive behaviors	USVs	Anxiety-like behaviors	Learning and memory	Other behavioral phenotypes	Biochemistry, morphology & structure	Shank expression	Synaptic function	
	coding exon 13 (exons 13-19 deletion)				arm in the elevated plus maze in heterozygous mice		auditory stimuli and locomotor activity • Significant decrease and increase in latency to fall in female KO and heterozygous mice, respectively, in the rotarod test	GluN2B, Homer1b/c, PSD-95, and Shank3 HMW • In hippocampal synaptosome preparation, decreases in GluA1 and GluN1 in heterozygous mice	of the lower two Shank3 isoforms	and PPR in the hippocampus • Decreased NMDA/AMPA ratio in the dorsal striatum	
	PDZ domain-coding exons 14–16 deletion (1 line)	• Normal in the three-chamber social interaction • Enhanced social dyadic	• Enhanced self-grooming without bedding • Enhanced self-grooming but reduced digging with bedding	• Suppressed USVs with a novel female stranger	• Normal time in the center in the open-field • More time spent in open arm in the elevated plus maze • Less time spent in the light chamber in light-dark test	N/A	• Novelty-induced hypoactivity	N/A	• Complete loss of Shank3a and Shank3c/d proteins in the thalamus, striatum, hippocampus, and cortex • Complete loss of Shank3e in the thalamus but not in the striatum, hippocampus, and cortex	• Suppressed excitatory synaptic transmission in the dorsolateral striatum	Yoo T et al., 2018
		N/A	N/A	N/A	N/A	N/A	N/A	N/A	N/A	• Increased excitability and altered excitatory and inhibitory spontaneous synaptic transmission in mPFC layer 2/3 pyramidal neurons	Yoo T et al., 2019
	PDZ domain-coding exons 14–16 deletion in GABAergic neurons	• Normal in the three-chamber social interaction • Enhanced social dyadic	• Normal self-grooming without bedding • Enhanced self-grooming but reduced digging with bedding	• Suppressed USVs with a novel female stranger	• Less time in the center in the open-field • Normal time spent in open arm in the elevated plus maze • Less time spent in the light chamber in light-dark test	N/A	• Novelty-induced hypoactivity	N/A	• Unaltered Shank3a, Shank3c/d, and Shank3e in the thalamus, hippocampus, and cortex • Significantly reduced Shank3a but unaltered Shank3c/d and Shank3e in the striatum	• Suppressed excitatory synaptic transmission in the dorsolateral striatum	Yoo T et al., 2018
	PDZ domain-coding exons 14–16 deletion	• Normal in the three-chamber social interaction	• Normal self-grooming without bedding • Modestly	• Normal USVs with a novel female stranger	• Normal time spent in the center in the open-field	N/A	• Normal locomotor activity	N/A	• Unaltered Shank3a, Shank3c/d, and Shank3e in the	• Increased excitability in mPFC layer 2/3 pyramidal neurons	Yoo T et al., 2019

(continued on next page)

Table 3 (continued)

Targeted scaffold protein	Mouse model details	Behavioral phenotypes						Non-behavioral phenotypes			References
		Social behaviors	Repetitive behaviors	USVs	Anxiety-like behaviors	Learning and memory	Other behavioral phenotypes	Biochemistry, morphology & structure	Shank expression	Synaptic function	
	in glutamatergic neurons	<ul style="list-style-type: none"> Enhanced social dyadic 	<ul style="list-style-type: none"> enhanced repetitive self-grooming with bedding, but normal digging with bedding 		<ul style="list-style-type: none"> More time spent in open arm in the elevated plus maze Normal time spent in the light chamber in light-dark test 				<ul style="list-style-type: none"> thalamus and striatum Significantly reduced Shank3a and Shank3c/d but not Shank3e in the hippocampus and cortex Unaltered Shank1 and Shank2 in the thalamus, striatum, hippocampus, and cortex 	<ul style="list-style-type: none"> Normal spontaneous excitatory and inhibitory synaptic transmission in mPFC layer 2/3 pyramidal and dorsolateral striatal neurons 	
	PRO domain-coding exon 21 deletion ($\Delta E21$, $\Delta C/\Delta C$)	<ul style="list-style-type: none"> Minimal social interaction deficit Normal social interaction with a juvenile conspecific mouse No preference for social novelty Normal avoidance of inanimate objects 	<ul style="list-style-type: none"> Increased grooming in older mice (10–13 months old) but not in younger mice Little to no interest in burying marbles 	<ul style="list-style-type: none"> No differences in the latency to emit the first call or the total number of calls in males with free-roaming estrous females 	<ul style="list-style-type: none"> Increased time spent in the dark and increased latency to the light side in light-dark test Normal anxiety-like behavior in the elevated plus maze and open-field Little to no interest in burying marbles 	<ul style="list-style-type: none"> Impaired spatial original learning but normal reversal learning in MWM 	<ul style="list-style-type: none"> Impaired motor coordination in rotarod Aberrant locomotor activity Hypersensitive in the hotplate task Impaired nest building Normal startle reactivity and PPI 	<ul style="list-style-type: none"> No morphological defects in dendritic complexity and spine density in CA1 neurons In the hippocampal whole lysates, no changes in synaptic proteins, including PSD-95, PSD-93, Homer, a-Fodrin, Neurexin, NL1, NL3, GluN1, GluN2A, GluN2B, GluA1, GluA2/3, mGluR1, and mGluR5 In the hippocampal synaptosomal and PSDII fractions, enhanced mGluR5 	<ul style="list-style-type: none"> Loss of major (largest three) Shank3 isoforms but increases of small-sized Shank3 isoforms in the hippocampal whole lysates (5–6 months old) No changes in Shank1 and Shank2 in the hippocampal whole lysates 	<ul style="list-style-type: none"> Increased mGluR5 Impaired hippocampal LTP but normal LTD and mGluR-LTD Decreased NMDA/AMPA ratio at SC-CA1 synapses Unaltered amplitude but decreased frequency of mEPSC No change in PPR Decreased input-output relationship 	Kouser et al., 2013
	Insertion mutation in PRO domain-coding exon 21 (InsG3728)	<ul style="list-style-type: none"> Normal social interaction Showed novelty avoidance phenotype Normal in preference for the social target 	<ul style="list-style-type: none"> Normal grooming Impaired marble burying 	N/A	<ul style="list-style-type: none"> Normal in the elevated plus maze and open-field No difference in time spent in dark versus light chamber but increased latency to the light chamber in the bright-dark task 	<ul style="list-style-type: none"> Mildly impaired spatial learning and memory in MWM 	<ul style="list-style-type: none"> Impaired motor learning and coordination in rotarod Impaired nest building Decreased locomotor activity in response to novelty or in novel open-field 	<ul style="list-style-type: none"> In the hippocampal whole lysates and synaptosomes, no changes in synaptic proteins, including PSD-95, Homer1b/c, GluA1, GluA2, GluN1, GluN2A, GluN2B, and mGluR5 	<ul style="list-style-type: none"> Complete loss of Shank3 isoforms detected between ~150 and 250 kD The unchanged expression level of a band sized around 75 kD 	<ul style="list-style-type: none"> Impaired hippocampal LTP by a single 1 s train at 100 Hz but not by 4 trains at 100 Hz for 1 s each, separated by 60 s Impaired hippocampal mGluR-LTD Decreased basal synaptic strength at SC-CA1 synapses 	Speed et al., 2015

(continued on next page)

Table 3 (continued)

Targeted scaffold protein	Mouse model details	Behavioral phenotypes						Non-behavioral phenotypes			References
		Social behaviors	Repetitive behaviors	USVs	Anxiety-like behaviors	Learning and memory	Other behavioral phenotypes	Biochemistry, morphology & structure	Shank expression	Synaptic function	
					<ul style="list-style-type: none"> Burying less marbles 					<ul style="list-style-type: none"> Unaffected PPR Decreased NMDA/AMPA ratio Decreased frequency but unaffected amplitude of mEPSC (In the striatum at P14) Reduced field population spikes Increased amplitude but unaltered frequency of mEPSC No change in NMDA/AMPA ratio Unaffected presynaptic function (In mPFC at P14) Unaltered mEPSC amplitude and frequency (In adult striatum) Reduced pop spike responses Unaffected presynaptic function Reduced mEPSC amplitude and frequency Reduced NMDA currents 	Zhou et al., 2016
	Insertion mutation in PRO domain-coding exon 21 (InsG3680)	<ul style="list-style-type: none"> Impaired social interaction and novelty Social dominance-like behavior 	<ul style="list-style-type: none"> Self-injurious grooming 	<ul style="list-style-type: none"> Normal in total number, total duration, mean duration, and peak amplitude of calls at P2 and P12 mice 	<ul style="list-style-type: none"> Increased anxiety level showing less time spent in exploring the center in an open area and in the open arms in the elevated zero maze 	<ul style="list-style-type: none"> Normal working memory in T-maze 	<ul style="list-style-type: none"> Reduced explorative activity in the open-field Impaired motor learning and coordination in rotaroad Defects in acoustic startle response Reduced PPI 	<ul style="list-style-type: none"> Reduced spine density in mPFC Upregulation of Shank1/2 mRNA in mPFC but not in the striatum Reduced Homer1b/c but increased GluA1 in striatum at P14 Reduced Homer1b/c, SAPAP3, SynGAP, GluN1, GluN2A, GluN2B, GluA2, and mGluR5 in adult striatum Reduced Homer1b/c, PSD-95, and PSD-93 in adult mPFC 	<ul style="list-style-type: none"> No Shank3 isoforms detected above 75 kD in the striatal PSD fraction 	<ul style="list-style-type: none"> Unaffected presynaptic function (In mPFC at P14) Unaltered mEPSC amplitude and frequency (In adult striatum) Reduced pop spike responses Unaffected presynaptic function Reduced mEPSC amplitude and frequency Reduced NMDA currents 	Zhou et al., 2016
	All domains-coding exons 4–22 deletion	<ul style="list-style-type: none"> Normal in bidirectional contact but prolonged in non-reciprocated interaction in the social dyadic test No preference for home nests Unstable dominance hierarchies 	<ul style="list-style-type: none"> Excessive self-injurious grooming Less engaged holes and great tendency to re-investigate the same hole in the hole-board exploration More self-grooming during the social test 	<ul style="list-style-type: none"> Fewer and shorter calls in pups at P4 and adults exposed to estrous females 	<ul style="list-style-type: none"> Increased anxiety-like behaviors in the open-field (spent less time in the center) and light-dark test (delayed entry into the light chamber) 	<ul style="list-style-type: none"> Normal original learning and impaired reversal learning in MWM task 	<ul style="list-style-type: none"> Impaired motor performance in rotarod Reduced locomotion and rearing in the open-field Enhanced reactivity to novel environments Reduced startle reactivity Intact fear learning but slightly enhanced 	<ul style="list-style-type: none"> Enlarged basal ganglia and thalamus with smaller olfactory areas, hippocampus, and amygdala Reduced spine density in the striatum but not in the hippocampus Shorter and thinner PSD of striatal synapses Decreased pan-SAPAP and 	<ul style="list-style-type: none"> No detection of all mRNA isoforms of <i>Shank3</i> Complete loss of all Shank3 isoform proteins 	<ul style="list-style-type: none"> Altered functional neural connectivity in a frontostriatal circuit Nucleus accumbens firing deficit Enhanced intrinsic excitability of MSNs Unaltered amplitude but reduced frequency of sEPSC in MSNs Impaired striatal LTD 	Wang et al., 2016

(continued on next page)

Table 3 (continued)

Targeted scaffold protein	Mouse model details	Behavioral phenotypes						Non-behavioral phenotypes			References	
		Social behaviors	Repetitive behaviors	USVs	Anxiety-like behaviors	Learning and memory	Other behavioral phenotypes	Biochemistry, morphology & structure	Shank expression	Synaptic function		
		<ul style="list-style-type: none"> • Normal sociability preference in the three-chamber 	<ul style="list-style-type: none"> • Excessive self-injurious grooming 	<ul style="list-style-type: none"> • Fewer calls and shorter call duration 	<ul style="list-style-type: none"> • Reduced anxiety-like behaviors in the elevated zero maze (more time spent in open areas) 	N/A	<ul style="list-style-type: none"> • Enhanced freezing for contextual fear • Augmented PPI • Reduced startle activity • Reduced locomotion and rearing in the open-field 	<ul style="list-style-type: none"> • Mildly perturbed hippocampal spatial memory • Severely impaired striatum-dependent instrumental learning 	<ul style="list-style-type: none"> • SAPAP3 levels only in the striatum • Reduced GluN2A only in the hippocampus • Homer1b/c decreased in the striatal PSD fraction and mildly reduced in the hippocampal PSD fraction • mGluR5 increased in the striatum but not in the hippocampus • Selective alterations of both mGluR5-Homer scaffolds and mGluR5-mediated signaling in striatal neurons • Reduced Homer1b/c in striatal loss of Shank3 • Increased NMDA receptor-currents and GluN2B-containing NMDA receptors in the loss of Shank3 in hippocampal neurons 	<ul style="list-style-type: none"> • (NEX-Shank3 mouse) • Loss of Shank3a protein in the cortex and hippocampus, but not in the striatum (crude PSD fractions) • Significantly increased Shank3c/d and Shank3e proteins in the hippocampus but unchanged in the cortex and striatum (Dlx5/6-Shank3 mouse) • Loss of Shank3a protein in the striatum but not in the cortex and hippocampus (crude PSD fractions) • Shank3c/d protein: 	<ul style="list-style-type: none"> • Increased NMDA/AMPA ratio in the loss of Shank3 in hippocampal neurons 	<ul style="list-style-type: none"> • Bey et al., 2018

(continued on next page)

Table 3 (continued)

Targeted scaffold protein	Mouse model details	Behavioral phenotypes						Non-behavioral phenotypes			References
		Social behaviors	Repetitive behaviors	USVs	Anxiety-like behaviors	Learning and memory	Other behavioral phenotypes	Biochemistry, morphology & structure	Shank expression	Synaptic function	
Shank1/ Shank3 (DKO)	Generated by crossing Shank1ΔE14-15 (Hung et al., 2008) and Shank3ΔE11 (Schmeisser et al., 2012)	<ul style="list-style-type: none"> • Impaired sociability and social novelty in the three-chamber 	<ul style="list-style-type: none"> • Increased repetitive self-grooming 	N/A	<ul style="list-style-type: none"> • Reduced anxiety-like behavior in the elevated plus maze 	<ul style="list-style-type: none"> • Impaired spatial object recognition and NOR • Impaired spatial original and reversal learning in T-maze and MWM 	<ul style="list-style-type: none"> • Impaired nest building • Impaired motor coordination in rotarod • Impaired in the balance beam test • Longer time spent in the pole test 	(at P22-25) <ul style="list-style-type: none"> • Reduced spine density and branching points in the cortex and hippocampus • Reduced PSD thickness and synapse number but unaltered PSD length in the cortex • Reduced PSD thickness and PSD length but unaffected synapse number in the hippocampus • Reduced mGluR5, Homer, Arc, p-ERK1/2, p-eEF2, p-Akt, and p-S6 in the cortex • Increased mGluR5 and reduced Arc, p- 	significantly increased in the striatum but unaltered in the cortex and hippocampus <ul style="list-style-type: none"> • Unaltered Shank3e protein in the cortex, hippocampus, and striatum (<i>Drd1-Shank3</i> or <i>Drd2-Shank3</i> mice) • Loss of Shank3a protein in the striatum but not in the cortex and hippocampus (crude PSD fractions) • Unaltered Shank3c/d and Shank3e proteins in the cortex, hippocampus, and striatum (at P22-25 & P60) <ul style="list-style-type: none"> • Almost complete loss of Shank1 and reduced or loss of some isoforms of Shank3 in the cortex and hippocampus (PSD-enriched fractions) • No compensatory increase in Shank2 in the cortex and hippocampus (PSD-enriched fractions) 	(at P60) <ul style="list-style-type: none"> • Normal HFS-LTP but impaired depotentiation at SC-CA1 synapses • Reduced LTP in DG • Increase in the number of spikes in EEG recording of freely moving mice • Unaltered sEPSC amplitude in both CA1 and DG neurons • sEPSCs frequency reduced in CA1 but increased in DG • Unaltered PPR 	Mossa et al., 2021

(continued on next page)

Table 3 (continued)

Targeted scaffold protein	Mouse model details	Behavioral phenotypes						Non-behavioral phenotypes			References	
		Social behaviors	Repetitive behaviors	USVs	Anxiety-like behaviors	Learning and memory	Other behavioral phenotypes	Biochemistry, morphology & structure	Shank expression	Synaptic function		
											eEF2, p-Akt, and p-S6 in the hippocampus <ul style="list-style-type: none"> • No alterations in GluN1, GluN2A, GluN2B, GluA1, and GluA2 in the cortex and hippocampus (at P60) • Reduced spine density, branching points, secondary dendrites and soma area in the cortex • Reduced spine density, but unaltered branching points, secondary dendrites and soma area in the hippocampus • Reduced mGluR5, Homer, p-ERK1/2, and p-S6 in the cortex but no alterations in the hippocampus 	

Abbreviations: ACC, anterior cingulate cortex; AMPA, L- α -amino-3-hydroxy-5-methyl-4-isoxazolepropionate; ANK, ankyrin repeat domain; DG, dentate gyrus; DKO, double knockout; EEG, electroencephalogram; E/I, excitation/inhibition; GABA, gamma-aminobutyric acid; GKAP, guanylate kinase-associated protein; HFS, high-frequency stimulation; HMW, high molecular weight; LTD, long-term depression; LTP, long-term potentiation; mEPSC, miniature excitatory postsynaptic current; mGluR, metabotropic glutamate receptor; mIPSC, miniature inhibitory postsynaptic current; mPFC, medial prefrontal cortex; MSNs, medium spiny neurons; MWM, Morris water maze; NMDA, N-methyl-d-aspartate; NL, Neuroligin; NOR, novel object recognition; N/A, not applicable as the experiment was not conducted; PDZ, PSD-95/Discs large/Zona occludens-1 domain; PPI, prepulse inhibition; PPR, paired-pulse ratio; PRO, proline-rich region; PSD, postsynaptic density; PSD-95, postsynaptic density protein 95; SAPAP, SAP90/PSD-95-associated protein; SC-CA1, Schaffer collateral-Cornu Ammonis 1; sEPSC, spontaneous excitatory postsynaptic current; Shank, SRC homology 3 (SH3) and multiple ankyrin repeat domain; SPM, synaptic plasma membrane; USVs; ultrasonic vocalizations; WT, wild-type.

observed [64]. In *Shank3*^{ΔE13–16} mutant mice, mEPSC amplitude and frequency were normal in the hippocampus but reduced in MSNs [25]. Specifically, reduced mEPSC frequency was observed in D2 (striato-pallidal indirect pathway) but not in D1 (striatonigral direct pathway) MSNs [75]. Decreased mEPSC amplitude and frequency, reduced AMPA/NMDA ratio, and no changes in PPR were observed in ACC pyramidal neurons in global KO *Shank3*^{ΔE13–16} mutant mice or mice with conditional *Shank3* deletion in the ACC [79]. Consistent with the mEPSC data, spine density was also reduced in the ACC pyramidal neurons in global KO *Shank3*^{ΔE13–16} mutant mice [79].

In *Shank3* complete KO (*Shank3*^{ΔE4–22}) mice that showed enhanced repetitive self-grooming, the expression level of mGluR5 in the striatal PSD fraction was increased [70]. Treatment with a selective mGluR5 antagonist, 2-methyl-6-(phenylethynyl)-pyridine (MPEP) or the mGluR5-positive allosteric modulator, 3-cyano-N-(1,3-diphenyl-1 H-pyrazol-5-yl) benzamide (CDPPB), suppressed or further augmented, respectively, the enhanced self-grooming observed in *Shank3*^{ΔE4–22} mice. These results indicate that the enhanced repetitive self-grooming observed in *Shank3*^{ΔE4–22} mice can be attributed to the increased level of mGluR5. The impaired instrumental learning observed in *Shank3*^{ΔE4–22} mice was partially rescued by treatment with CDPPB [70], indicating that instrumental learning is dependent on mGluR5 functionality. As we have described, both different and the same *Shank3* mutant lines show various behavioral, biochemical, structural, and physiological phenotypes, supporting that Shank3 isoforms play differential roles in the pathological mechanisms underlying ASD in a brain region-, circuit-, and/or developmental stage-dependent manner.

2.6. *Shank1/Shank3* double KO mutant mice associated with ASD

Since the deletion of one out of three Shank proteins, Shank1, Shank2, and Shank3, could induce compensatory functions covered by the other remaining Shank proteins [60,69], the generation of mutant mice, in which all three *Shank* genes are simultaneously deleted, is ideal to fully understand the function of Shank protein. However, complete KO of all three *Shank* genes may be lethal to mice at the embryonic stage. Recently, *Shank1*^{-/-}/*Shank3*^{-/-} double KO (DKO) mice were generated by crossing *Shank1*^{ΔE14–15} [53] and *Shank3*^{ΔE11} [60,76] mutant mice [80]. *Shank1*^{-/-}/*Shank3*^{-/-} DKO mice, which have a much lower survival rate and slightly smaller body and brain sizes compared to those of WT mice, displayed severe behavioral impairments, including impaired sociability and social novelty in the three-chamber test, increased repetitive self-grooming, decreased anxiety-like behavior in an elevated plus maze, and impaired motor coordination and balance in the rotarod, beam, and pole tests [80]. In addition, spatial original and reversal learning functions were also impaired in the T-maze and MWM tasks [80].

Shank1^{-/-}/*Shank3*^{-/-} DKO mice showed altered neuronal morphology and molecular compositions that differed between developing (P22–25) and adult (P60) mice. Reduced spine density was observed in the cortex and hippocampus of P22–25 and P60 DKO mice, while reduced dendritic branching points were observed in the cortex and hippocampus of P22–25 mice and in the cortex but not in the hippocampus of P60 DKO mice [80]. In developing DKO mice at P22–25, the expression levels of synaptic and intracellular signaling molecules, including mGluR5, Homer, Arc, p-ERK1/2, p-eEF2, p-Akt, and p-S6, were decreased in the cortex. On the other hand, increased mGluR5 and decreased Arc, p-eEF2, p-Akt, and p-S6 levels were observed in the hippocampus. In adult DKO mice at P60, the expression levels of mGluR5, Homer, p-ERK1/2, and p-S6 were reduced in the cortex but not altered in the hippocampus [80]. In adult DKO mice, normal LTP but impaired depotentiation were observed at Schaffer collateral-CA1 synapses, while reduced LTP was observed in the dentate gyrus [80]. The reduced p-Akt level observed in the developing mice can be pharmacologically rescued by chronic treatment with cotinine, which is the major metabolite of nicotine and is known to increase Akt phosphorylation and improve

cognitive function in rodents [81,82]. Cotinine treatment from P14 to P30, a critical period for neural maturation and circuit formation, rescued the neuronal morphological changes and behavioral deficits observed in the DKO mice [80]. These findings indicate that Akt and its intracellular signaling are regulated by Shank1 and Shank3, and contribute to brain development, synaptic plasticity, and behaviors related to ASD and cognition.

3. Discussion

Many *Shank* mutant mice, including *Shank1* (one line), *Shank2* (two lines), and *Shank3* (more than 14 lines) mutants, have been generated to investigate the function of Shank proteins in ASD (Tables 1–3). The symptoms of ASD in mouse models include various behavioral deficits in social interaction, repetitive behavior, USVs, anxiety-like behaviors, learning and memory, and cognitive flexibility. However, as we described in this review, *Shank* mutant mice do not exhibit all the defective behavioral phenotypes associated with ASD; rather, some mouse lines only exhibit parts of defective phenotypes, while some display distinct phenotypes. For instance, in the case of studies using several *Shank3* mutant mice or even the same mutant line, the results obtained from the same behavioral experiments were largely various. In addition, *Shank3* mutant mice, even those with deletions of the same exons, exhibit different behavioral phenotypes. Furthermore, synaptic structure and function affected in different *Shank3* mutant mice were also various. The isoforms deleted in mice, the ages of the mice subjected to experiments, and the experience of mice before the behavioral test in case the mice were subjected to several behavioral tests sequentially would be critical factors to consider when interpreting data showing various behavioral phenotypes obtained from the same *Shank3* mutant line. In addition, the differences in the gene products from the deletions/mutations in the same exons of *Shank3* could cause distinct phenotypes in the synaptic structure and function and behaviors in *Shank3* mutant mice. Two *Shank3* mutant lines, *Shank3*^{InsG3680} and *Shank3*^{R1117X}, which have mutations in the same exon (exon 21), showed the complete loss of Shank3 protein and a truncated Shank3 protein, respectively [69]. Indeed, the difference in the Shank3 gene product (i.e., no expression of Shank3 protein vs a truncated form of Shank3 protein expression) may explain the differential synaptic and behavioral phenotypes observed in those two *Shank3* mutant lines. Besides genetic factors, the different phenotypes in synapses and behaviors in *Shank3* mutant mice can partly be accounted for by environmental factors, including paternal and maternal age, maternal physical and mental health, and birth order and complications [83–88].

There appears to be a consensus that the generation of mutant mice, in which two *Shank* genes out of *Shank1*, *Shank2*, and *Shank3* are simultaneously deleted, seems necessary to further elucidate the role of Shank proteins in ASD [80]. In addition to Shank proteins, PSD-95, which forms a postsynaptic complex with Shank proteins via SAPAP/GKAP (Fig. 1), was also revealed as another postsynaptic scaffolding protein in which genetic mutations were identified in patients with ASD [6]. PSD-95 KO mice displayed autism-related behavioral phenotypes, including social deficits, increased repetitive behavior, reduced vocalization, impaired motor coordination, and anxiety-related responses [29]. It is plausible that the generation of a DKO mouse model targeting essential genes in PSD scaffolding proteins, such as Shank and PSD-95, associated with ASD could help to dissect the molecular and cellular mechanisms that underlie extremely complicated ASD and could provide new insights into the field of ASD and new targets for therapeutic strategies.

Several recent studies have demonstrated that certain autistic behaviors are selectively reversed by Shank re-expression at embryonic, juvenile, and adult stages [74,79,84,89,90]. Re-expression of Shank3 in adult *Shank3*^{fx/fx} mutant mice rescued social interaction deficits and repetitive grooming behavior [74]. In addition, selective re-expression of Shank3 in the ACC of adult *Shank3*^{ΔE13–16} KO mice only rescued

social interaction deficits [79]. Restoration of Shank3 in germline and juvenile *Shank3^{fx/fx}* mutant mice reversed anxiety-like behavior and motor coordination deficits [74]. Early embryonic restoration of Shank3 in *Shank3* mutant (*Shank3^{ΔE13-19}*) mice rescued social interaction deficits and repetitive grooming [90]. Besides Shank3 re-expression, autistic behavioral phenotypes were also rescued by treatment with a potent histone deacetylase inhibitor [91] or by improved sleep [92]. Together, these studies imply promising translational approaches that Shank3, epigenetic and environmental factors, and critical temporal windows of developmental stages could be possible targets for the development of therapeutics for ASD. Nevertheless, there is still a long way to go. For ASD therapeutics to come to fruition, it is critical to identify (for example, Shank3-mediated) the detailed cellular and molecular mechanisms that underlie the behavioral pathophysiological phenotypes of ASD in a developmental stage-specific manner, which could provide precise information for application in pharmacological development toward translational studies. Regarding the safety aspect of the translational approach, further establishment of non-human primate ASD models [93] and intensive studies using them should also be conducted.

Recently, high-end omics technology, including next-generation sequencing, has been applied in various fields, including neurobiology and neurological disorders. An increasing number of studies using proteomic analysis have revealed a correlation between the changing interactome in PSD and psychiatric disorders [94–96]. In addition to protein-level proteomic studies, large-scale genomic data, including exome sequencing, ribonucleic acid (RNA) sequencing, and single-cell RNA sequencing [6–9, 47, 97], were obtained from disease mouse models or patients. This helps provide information on the mutations and target molecules and identify the specific brain regions, cell types, and/or circuitry responsible for the corresponding neurodevelopmental disorders.

Neurodevelopmental disorders, including ASD, schizophrenia, ADHD, and bipolar disorders, share many risk genes and have several shared and distinct symptoms [69, 98–100]. Indeed, a study reported that two *Shank3* mutant lines linked to ASD (*Shank3^{InsG3680}*) and schizophrenia (*Shank3^{R1117A}*) show not only shared but also distinct molecular, synaptic, circuit, and behavioral defects [69]. As discussed in this review, ASD mouse models exhibit a very wide range of phenotypical severity in each behavioral test, which is reminiscent of ASD patients with their own severity levels, from normal to very severe, for each symptom. Due to the extremely spectral and diverse features of ASD symptoms among patients, personalized therapeutic strategies may need to be considered. Therefore, symptom-based strategies combined with personalized medicine may be a good choice for ASD treatment. Furthermore, considering that neurodevelopmental disorders have some risk genes, pathologies, and symptoms in common, intensive mechanistic studies that target specific symptoms would be beneficial in that they could provide valuable delicate information on the diagnosis and treatment of individual patients with such symptoms in various neurodevelopmental disorders.

Funding

The work in the Park laboratory was supported by the Original Technology Research Program for Brain Science of the National Research Foundation of Korea (NRF) funded by the Korean government (MSIT) (NRF-2018M3C7A1021848 and NRF-2021R1A2C2004606) and KIST Institutional Program (2E31512).

CRediT authorship contribution statement

M.P. conceptualized the study. S.J. and M.P. wrote the manuscript and approved it for publication.

Declaration of Competing Interest

The authors declare that they have no conflicts of interest.

Data availability

Data will be made available on request.

References

- [1] J.T. Ting, J. Peca, G. Feng, Functional consequences of mutations in postsynaptic scaffolding proteins and relevance to psychiatric disorders, *Annu Rev. Neurosci.* 35 (2012) 49–71.
- [2] B.A. Jordan, B.D. Fernholz, M. Boussac, C. Xu, G. Grigorean, E.B. Ziff, T. A. Neubert, Identification and verification of novel rodent postsynaptic density proteins, *Mol. Cell Proteom.* 3 (9) (2004) 857–871.
- [3] J. Peng, M.J. Kim, D. Cheng, D.M. Duong, S.P. Gygi, M. Sheng, Semiquantitative proteomic analysis of rat forebrain postsynaptic density fractions by mass spectrometry, *J. Biol. Chem.* 279 (20) (2004) 21003–21011.
- [4] M. Sheng, C.C. Hoogenraad, The postsynaptic architecture of excitatory synapses: a more quantitative view, *Annu Rev. Biochem.* 76 (2007) 823–847.
- [5] S. Berkel, C.R. Marshall, B. Weiss, J. Howe, R. Roeth, U. Moog, V. Endris, W. Roberts, P. Szatmari, D. Pinto, M. Bonin, A. Riess, H. Engels, R. Sprengel, S. W. Scherer, G.A. Rappold, Mutations in the SHANK2 synaptic scaffolding gene in autism spectrum disorder and mental retardation, *Nat. Genet.* 42 (6) (2010) 489–491.
- [6] S. De Rubeis, X. He, A.P. Goldberg, C.S. Poultnery, K. Samocha, A.E. Cicek, Y. Kou, L. Liu, M. Fromer, S. Walker, T. Singh, L. Klei, J. Kosmicki, F. Shih-Chen, B. Alekic, M. Biscaldi, P.F. Bolton, J.M. Brownfeld, J. Cai, N.G. Campbell, A. Carracedo, M.H. Chahrour, A.G. Chiocchetti, H. Coon, E.L. Crawford, S. R. Curran, G. Dawson, E. Duketis, B.A. Fernandez, L. Gallagher, E. Geller, S. J. Guter, R.S. Hill, J. Ionita-Laza, P. Jimenez Gonzalez, H. Kilpinen, S.M. Klauck, A. Kolevzon, I. Lee, I. Lei, J. Lei, T. Lehtimaki, C.F. Lin, A. Ma'ayan, C. R. Marshall, A.L. McInnes, B. Neale, M.J. Owen, N. Ozaki, M. Parellada, J.R. Parr, S. Purcell, K. Puura, D. Rajagopalan, K. Rehnstrom, A. Reichenberg, A. Sabo, M. Sachse, S.J. Sanders, C. Schafer, M. Schulte-Ruther, D. Skuse, C. Stevens, P. Szatmari, K. Tammimies, O. Valladares, A. Voran, W. Li-San, L.A. Weiss, A. J. Willsey, T.W. Yu, R.K. Yuen, D.D.D. Study, A. Homozygosity Mapping Collaborative for, U.K. Consortium, E.H. Cook, C.M. Freitag, M. Gill, C. M. Hultman, T. Lehner, A. Palotie, G.D. Schellenberg, P. Sklar, M.W. State, J. S. Ruedcliffe, C.A. Walsh, S.W. Scherer, M.E. Zwick, J.C. Barrett, D.J. Cutler, K. Roeder, B. Devlin, M.J. Daly, J.D. Buxbaum, Synaptic, transcriptional and chromatin genes disrupted in autism, *Nature* 515 (7526) (2014) 209–215.
- [7] M. Fromer, A.J. Pocklington, D.H. Kavanagh, H.J. Williams, S. Dwyer, P. Gormley, L. Georgieva, E. Rees, P. Palta, D.M. Ruderfer, N. Carrera, I. Humphreys, J.S. Johnson, P. Roussos, D.D. Barker, E. Banks, V. Milanova, S. G. Grant, E. Hannon, S.A. Rose, K. Chambert, M. Mahajan, E.M. Scolnick, J. L. Moran, G. Kirov, A. Palotie, S.A. McCarroll, P. Holmans, P. Sklar, M.J. Owen, S. M. Purcell, M.C. O'Donovan, De novo mutations in schizophrenia implicate synaptic networks, *Nature* 506 (7487) (2014) 179–184.
- [8] I. Iossifov, B.J. O'Roak, S.J. Sanders, M. Ronemus, N. Krumm, D. Levy, H. A. Stessman, K.T. Witherspoon, L. Vives, K.E. Patterson, J.D. Smith, B. Paepier, D. A. Nickerson, J. Dea, S. Dong, L.E. Gonzalez, J.D. Mandell, S.M. Mane, M. T. Murtha, C.A. Sullivan, M.F. Walker, Z. Waqar, L. Wei, A.J. Willsey, B. Yamrom, Y.H. Lee, E. Grabowska, E. Dalkic, Z. Wang, S. Marks, P. Andrews, A. Leotta, J. Kendall, I. Hakker, J. Rosenbaum, B. Ma, L. Rodgers, J. Troge, G. Narzisi, S. Yeon, M.C. Schatz, K. Ye, W.R. McCombie, J. Shendure, E.E. Eichler, M. W. State, M. Wigler, The contribution of de novo coding mutations to autism spectrum disorder, *Nature* 515 (7526) (2014) 216–221.
- [9] S.M. Purcell, J.L. Moran, M. Fromer, D. Ruderfer, N. Solovieff, P. Roussos, C. O'Dushlaine, K. Chambert, S.E. Bergen, A. Kahler, L. Duncan, E. Stahl, G. Genovese, E. Fernandez, M.O. Collins, N.H. Komiyama, J.S. Choudhary, P. K. Magnusson, E. Banks, K. Shakir, K. Garimella, T. Fennell, M. DePristo, S. G. Grant, S.J. Haggarty, S. Gabriel, E.M. Scolnick, E.S. Lander, C.M. Hultman, P. F. Sullivan, S.A. McCarroll, P. Sklar, A polygenic burden of rare disruptive mutations in schizophrenia, *Nature* 506 (7487) (2014) 185–190.
- [10] D. Sato, A.C. Lionel, C.S. Leblond, A. Prasad, D. Pinto, S. Walker, I. O'Connor, C. Russell, I.E. Drmic, F.F. Hamdan, J.L. Michaud, V. Endris, R. Roeth, R. Delorme, G. Huguette, M. Leboyer, M. Rastam, C. Gillberg, M. Lathrop, D. J. Stavropoulos, E. Anagnostou, R. Weksberg, E. Fombonne, L. Zwaigenbaum, B. A. Fernandez, W. Roberts, G.A. Rappold, C.R. Marshall, T. Bourgeron, P. Szatmari, S.W. Scherer, SHANK1 deletions in males with autism spectrum disorder, *Am. J. Hum. Genet.* 90 (5) (2012) 879–887.
- [11] C. Schizophrenia Working Group of the Psychiatric Genomics, Biological insights from 108 schizophrenia-associated genetic loci, *Nature* 511 (7510) (2014) 421–427.
- [12] M.J. Maenner, K.A. Shaw, J. Baio, EdS, A. Washington, M. Patrick, M. DiRienzo, D.L. Christensen, L.D. Wiggins, S. Pettygrove, J.G. Andrews, M. Lopez, A. Hudson, T. Baroud, Y. Schwenk, T. White, C.R. Rosenberg, L.C. Lee, R.A. Harrington, M. Huston, A. Hewitt, Ph.D., A. Esler, J. Hall-Lande, J.N. Poynter, L. Hallas-Muchow, J.N. Constantino, R.T. Fitzgerald, W. Zahorodny, J. Shenouda, J.L. Daniels, Z. Warren, A. Vehorn, A. Salinas, M.S. Durkin, P.M. Dietz, Prevalence of Autism Spectrum Disorder Among Children Aged 8 Years - Autism and Developmental

- Disabilities Monitoring Network, 11 Sites, United States, 2016, MMWR Surveill Summ 69(4) (2020) 1–12.
- [13] A.P. Association. Diagnostic and statistical manual of mental disorders, 5th ed., American Psychiatric Association, 2013.
- [14] J.L. Silverman, A. Thurm, S.B. Ethridge, M.M. Soller, S.P. Petkova, T. Abel, M. D. Bauman, E.S. Brodtkin, H. Harony-Nicolas, M. Wöhr, A. Halladay, Reconsidering animal models used to study autism spectrum disorder: Current state and optimizing future, *Genes Brain Behav.* 21 (5) (2022), e12803.
- [15] J. Gauthier, T.J. Siddiqui, P. Huashan, D. Yokomaku, F.F. Hamdan, N. Champagne, M. Lapointe, D. Spiegelman, A. Noreau, R.G. Lafreniere, F. Fathalli, R. Joober, M.O. Krebs, L.E. DeLisi, L. Motttron, E. Fombonne, J. L. Michaud, P. Drapeau, S. Carbonetto, A.M. Craig, G.A. Rouleau, Truncating mutations in NRXN2 and NRXN1 in autism spectrum disorders and schizophrenia, *Hum. Genet* 130 (4) (2011) 563–573.
- [16] H.G. Kim, S. Kishikawa, A.W. Higgins, I.S. Seong, D.J. Donovan, Y. Shen, E. Lally, L.A. Weiss, J. Najm, K. Kutsche, M. Descartes, L. Holt, S. Braddock, R. Troxell, L. Kaplan, F. Volkmar, A. Klin, K. Tsatsanis, D.J. Harris, I. Noens, D.L. Pauls, M. J. Daly, M.E. MacDonald, C.C. Morton, B.J. Quade, J.F. Gusella, Disruption of neurexin 1 associated with autism spectrum disorder, *Am. J. Hum. Genet* 82 (1) (2008) 199–207.
- [17] A.K. Vaags, A.C. Lionel, D. Sato, M. Goodenberger, Q.P. Stein, S. Curran, C. Ogilvie, J.W. Ahn, I. Drmic, L. Senman, C. Chrysler, A. Thompson, C. Russell, A. Prasad, S. Walker, D. Pinto, C.R. Marshall, D.J. Stavropoulos, L. Zwaigenbaum, B.A. Fernandez, E. Fombonne, P.F. Bolton, D.A. Collier, J.C. Hodge, W. Roberts, P. Szatmari, S.W. Scherer, Rare deletions at the neurexin 3 locus in autism spectrum disorder, *Am. J. Hum. Genet* 90 (1) (2012) 133–141.
- [18] J.T. Glessner, K. Wang, G. Cai, O. Korvatska, C.E. Kim, S. Wood, H. Zhang, A. Estes, C.W. Brune, J.P. Bradfield, M. Imielinski, E.C. Frackelton, J. Reichert, E. L. Crawford, J. Munson, P.M. Sleiman, R. Chiavacci, K. Annaiah, K. Thomas, C. Hou, W. Glaberson, J. Flory, F. Otieno, M. Garris, L. Soorya, L. Klei, J. Piven, K. J. Meyer, E. Anagnostou, T. Sakurai, R.M. Game, D.S. Rudd, D. Zurawiecki, C. J. McDougle, L.K. Davis, J. Miller, D.J. Posey, S. Michaels, A. Kolevzon, J. M. Silverman, R. Bernier, S.E. Levy, R.T. Schultz, G. Dawson, T. Owley, W. M. McMahon, T.H. Wassink, J.A. Sweeney, J.I. Nurnberger, H. Coon, J. S. Sutcliffe, N.J. Minshew, S.F. Grant, M. Bucan, E.H. Cook, J.D. Buxbaum, B. Devlin, G.D. Schellenberg, H. Hakonarson, Autism genome-wide copy number variation reveals ubiquitin and neuronal genes, *Nature* 459 (7246) (2009) 569–573.
- [19] S. Jamain, H. Quach, C. Betancur, M. Rastam, C. Colineaux, I.C. Gillberg, H. Soderstrom, B. Giros, M. Leboyer, C. Gillberg, T. Bourgeron, S. Paris, Autism Research International Sibpair, Mutations of the X-linked genes encoding neurologins NLGN3 and NLGN4 are associated with autism, *Nat. Genet* 34 (1) (2003) 27–29.
- [20] T.C. Sudhof, Neurologins and neurexins link synaptic function to cognitive disease, *Nature* 455 (7215) (2008) 903–911.
- [21] A. Delahaye, A. Toutain, A. Aboura, C. Dupont, A.C. Tabet, B. Benzacken, J. Elion, A. Verloes, E. Pipiras, S. Drunat, Chromosome 22q13.3 deletion syndrome with a de novo interstitial 22q13.3 cryptic deletion disrupting SHANK3, *Eur. J. Med. Genet* 52 (5) (2009) 328–332.
- [22] C.M. Durand, C. Betancur, T.M. Boeckers, J. Bockmann, P. Chaste, F. Fauchereau, G. Nygren, M. Rastam, I.C. Gillberg, H. Anckarsater, E. Sponheim, H. Goubran-Botros, R. Delorme, N. Chabane, M.C. Mouren-Simeoni, P. de Mas, E. Bieth, B. Roge, D. Heron, L. Burglen, C. Gillberg, M. Leboyer, T. Bourgeron, Mutations in the gene encoding the synaptic scaffolding protein SHANK3 are associated with autism spectrum disorders, *Nat. Genet* 39 (1) (2007) 25–27.
- [23] J. Gauthier, D. Spiegelman, A. Piton, R.G. Lafreniere, S. Laurent, J. St-Onge, L. Lapointe, F.F. Hamdan, P. Cossette, L. Motttron, E. Fombonne, R. Joober, C. Marineau, P. Drapeau, G.A. Rouleau, Novel de novo SHANK3 mutation in autistic patients, *Am. J. Med. Genet B Neuropsychiatr. Genet* 150B (3) (2009) 421–424.
- [24] R. Moessner, C.R. Marshall, J.S. Sutcliffe, J. Skaug, D. Pinto, J. Vincent, L. Zwaigenbaum, B. Fernandez, W. Roberts, P. Szatmari, S.W. Scherer, Contribution of SHANK3 mutations to autism spectrum disorder, *Am. J. Hum. Genet* 81 (6) (2007) 1289–1297.
- [25] J. Peca, C. Feliciano, J.T. Ting, W. Wang, M.F. Wells, T.N. Venkatraman, C. D. Lascola, Z. Fu, G. Feng, Shank3 mutant mice display autistic-like behaviours and striatal dysfunction, *Nature* 472 (7344) (2011) 437–442.
- [26] J.L. Silverman, S.M. Turner, C.L. Barkan, S.S. Tolu, R. Saxena, A.Y. Hung, M. Sheng, J.N. Crawley, Sociability and motor functions in Shank1 mutant mice, *Brain Res.* 1380 (2011) 120–137.
- [27] X. Wang, P.A. McCoy, R.M. Rodriguiz, Y. Pan, H.S. Je, A.C. Roberts, C.J. Kim, J. Berrios, J.S. Colvin, D. Bousquet-Moore, I. Lorenzo, G. Wu, R.J. Weinberg, M. D. Ehlers, B.D. Philpot, A.L. Beaudet, W.C. Wetsel, Y.H. Jiang, Synaptic dysfunction and abnormal behaviors in mice lacking major isoforms of Shank3, *Hum. Mol. Genet* 20 (15) (2011) 3093–3108.
- [28] M. Wöhr, F.I. Rouillet, A.Y. Hung, M. Sheng, J.N. Crawley, Communication impairments in mice lacking Shank1: reduced levels of ultrasonic vocalizations and scent marking behavior, *PLoS One* 6 (6) (2011), e20631.
- [29] M. Feyder, R.M. Karlsson, P. Mathur, M. Lyman, R. Bock, R. Momenan, J. Munasinghe, M.L. Scattoni, J. Ihne, M. Camp, C. Graybeal, D. Strathdee, A. Begg, V.A. Alvarez, P. Kirsch, M. Rietschel, S. Cichon, H. Walter, A. Meyer-Lindenberg, S.G. Grant, A. Holmes, Association of mouse Dlg4 (PSD-95) gene deletion and human DLG4 gene variation with phenotypes relevant to autism spectrum disorders and Williams' syndrome, *Am. J. Psychiatry* 167 (12) (2010) 1508–1517.
- [30] C.S. Leblond, C. Nava, A. Polge, J. Gauthier, G. Huguet, S. Lumbroso, F. Giuliano, C. Stordeur, C. Depienne, K. Mouzat, D. Pinto, J. Howe, N. Lemiere, C.M. Durand, J. Guibert, E. Ey, R. Toro, H. Peyre, A. Mathieu, F. Amsellem, M. Rastam, I. C. Gillberg, G.A. Rappold, R. Holt, A.P. Monaco, E. Maestrini, P. Galan, D. Heron, A. Jacquette, A. Afenjar, A. Rastetter, A. Brice, F. Devillard, B. Assouline, F. Laffargue, J. Lespinasse, J. Chiesa, F. Rivier, D. Bonneau, B. Regnault, D. Zelenika, M. Delepine, M. Lathrop, D. Sanlaville, C. Schluth-Bolard, P. Edery, L. Perrin, A.C. Tabet, M.J. Schmeisser, T.M. Boeckers, M. Coleman, D. Sato, P. Szatmari, S.W. Scherer, G.A. Rouleau, C. Betancur, M. Leboyer, C. Gillberg, R. Delorme, T. Bourgeron, Meta-analysis of SHANK Mutations in Autism Spectrum Disorders: a gradient of severity in cognitive impairments, *PLoS Genet* 10 (9) (2014), e1004580.
- [31] D. Pinto, A.T. Pagnamenta, L. Klei, R. Anney, D. Merico, R. Regan, J. Conroy, T. R. Magalhaes, C. Correia, B.S. Abrahams, J. Almeida, E. Bacchelli, G.D. Bader, A. J. Bailey, G. Baird, A. Battaglia, T. Berney, N. Bolshakova, S. Bolte, P.F. Bolton, T. Bourgeron, S. Brennan, J. Brian, S.E. Bryson, A.R. Carson, G. Casallo, J. Casey, B.H. Chung, L. Cochrane, C. Corsello, E.L. Crawford, A. Crossett, C. Cyttrynbaum, G. Dawson, M. de Jonge, R. Delorme, I. Drmic, E. Duketus, F. Duque, A. Estes, P. Farrar, B.A. Fernandez, S.E. Folstein, E. Fombonne, C.M. Freitag, J. Gilbert, C. Gillberg, J.T. Glessner, J. Goldberg, A. Green, J. Green, S.J. Guter, H. Hakonarson, E.A. Heron, M. Hill, R. Holt, J.L. Howe, G. Hughes, V. Hus, R. Iglizoi, C. Kim, S.M. Klauck, A. Kolevzon, O. Korvatska, V. Kustanovich, C. M. Lajonchere, J.A. Lamb, M. Laskawiec, M. Leboyer, A. Le Couteur, B. L. Leventhal, A.C. Lionel, X.Q. Liu, C. Lord, L. Lotspeich, S.C. Lund, E. Maestrini, W. Mahoney, C. Mantoulan, C.R. Marshall, H. McConachie, C.J. McDougle, J. McGrath, W.M. McMahon, A. Merikangas, O. Migita, N.J. Minshew, G.K. Mirza, J. Munson, S.F. Nelson, C. Noakes, A. Noor, G. Nygren, G. Oliveira, K. Papanikolaou, J.R. Parr, B. Parrini, T. Paton, A. Pickles, M. Pilsorge, J. Piven, C. P. Ponting, D.J. Posey, A. Poustka, F. Poustka, A. Prasad, J. Ragoussis, K. Renshaw, J. Rickaby, W. Roberts, K. Roeder, B. Roge, M.L. Rutter, L.J. Bierut, J.P. Rice, J. Salt, K. Sansom, D. Sato, R. Segurado, A.F. Sequeira, L. Senman, N. Shah, V.C. Sheffield, L. Soorya, I. Sousa, O. Stein, N. Sykes, V. Stopponi, C. Strawbridge, R. Tancredi, K. Tansey, B. Thiruvahindrapuram, A.P. Thompson, S. Thomson, A. Tryfon, J. Tsiantis, H. Van Engeland, J.B. Vincent, F. Volkmar, S. Wallace, K. Wang, Z. Wang, T.H. Wassink, C. Webber, R. Weksberg, K. Wing, K. Wittmeyer, S. Wood, J. Wu, B.L. Yaspan, D. Zurawiecki, L. Zwaigenbaum, J. D. Buxbaum, R.M. Cantor, E.H. Cook, H. Coon, M.L. Cuccaro, B. Devlin, S. Ennis, L. Gallagher, D.H. Geschwind, M. Gill, J.L. Haines, J. Hallmayer, J. Miller, A. P. Monaco, J.I. Nurnberger Jr., A.D. Paterson, M.A. Pericak-Vance, G. D. Schellenberg, P. Szatmari, A.M. Vicente, V.J. Vieland, E.M. Wijsman, S. W. Scherer, J.S. Sutcliffe, C. Betancur, Functional impact of global rare copy number variation in autism spectrum disorders, *Nature* 466 (7304) (2010) 368–372.
- [32] T. Wang, H. Guo, B. Xiong, H.A. Stessman, H. Wu, B.P. Coe, T.N. Turner, Y. Liu, W. Zhao, K. Hoekzema, L. Vives, L. Xia, M. Tang, J. Ou, B. Chen, Y. Shen, G. Xun, M. Long, J. Lin, Z.N. Kronenberg, Y. Peng, T. Bai, H. Li, X. Ke, Z. Hu, J. Zhao, X. Zou, K. Xia, E.E. Eichler, De novo genetic mutations among a Chinese autism spectrum disorder cohort, *Nat. Commun.* 7 (2016) 13316.
- [33] S. Naisbitt, E. Kim, J.C. Tu, B. Xiao, C. Sala, J. Valtschanoff, R.J. Weinberg, P. F. Worley, M. Sheng, Shank, a novel family of postsynaptic density proteins that binds to the NMDA receptor/PSD-95/GKAP complex and cortactin, *Neuron* 23 (3) (1999) 569–582.
- [34] T.M. Bockers, M.G. Mameza, M.R. Kreutz, J. Bockmann, C. Weise, F. Buck, D. Richter, E.D. Gundelfinger, H.J. Krienkamp, Synaptic scaffolding proteins in rat brain. Ankyrin repeats of the multidomain Shank protein family interact with the cytoskeletal protein alpha-fodrin, *J. Biol. Chem.* 276 (43) (2001) 40104–40112.
- [35] Y.H. Jiang, M.D. Ehlers, Modeling autism by SHANK gene mutations in mice, *Neuron* 78 (1) (2013) 8–27.
- [36] T. Uemura, H. Mori, M. Mishina, Direct interaction of GluRdelta2 with Shank scaffold proteins in cerebellar Purkinje cells, *Mol. Cell Neurosci.* 26 (2) (2004) 330–341.
- [37] T.M. Boeckers, C. Winter, K.H. Smalla, M.R. Kreutz, J. Bockmann, C. Seidenbecher, C.C. Garner, E.D. Gundelfinger, Proline-rich synapse-associated proteins ProSAP1 and ProSAP2 interact with synaptic proteins of the SAPAP/GKAP family, *Biochem Biophys. Res Commun.* 264 (1) (1999) 247–252.
- [38] H.J. Krienkamp, Scaffolding proteins at the postsynaptic density: shank as the architectural framework, *Handb. Exp. Pharm.* 186 (2008) 365–380.
- [39] J.C. Tu, B. Xiao, S. Naisbitt, J.P. Yuan, R.S. Petralia, P. Brakeman, A. Doan, V. K. Aakalu, A.A. Lanahan, M. Sheng, P.F. Worley, Coupling of mGluR/Homer and PSD-95 complexes by the Shank family of postsynaptic density proteins, *Neuron* 23 (3) (1999) 583–592.
- [40] L. Chen, D.M. Chetkovich, R.S. Petralia, N.T. Sweeney, Y. Kawasaki, R. J. Wenthold, D.S. Brecht, R.A. Nicoll, Stargazin regulates synaptic targeting of AMPA receptors by two distinct mechanisms, *Nature* 408 (6815) (2000) 936–943.
- [41] H.C. Kornau, L.T. Schenker, M.B. Kennedy, P.H. Seeburg, Domain interaction between NMDA receptor subunits and the postsynaptic density protein PSD-95, *Science* 269 (5231) (1995) 1737–1740.
- [42] M.C. Phelan, R.C. Rogers, R.A. Saul, G.A. Stapleton, K. Sweet, H. McDermid, S. R. Shaw, J. Claytor, J. Willis, D.P. Kelly, 22q13 deletion syndrome, *Am. J. Med Genet* 101 (2) (2001) 91–99.
- [43] M.C. Bonaglia, R. Giorda, R. Borgatti, G. Felisari, C. Gagliardi, A. Selicorni, O. Zuffardi, Disruption of the ProSAP2 gene in a t(12;22)(q24.1;q13.3) is associated with the 22q13.3 deletion syndrome, *Am. J. Hum. Genet* 69 (2) (2001) 261–268.

- [44] F.B. Cristian, A. Koppel, J. Janssen, J.S. Utikal, G.A. Rappold, S. Berkel, Generation of two hiPSC lines from a patient with autism spectrum disorder harboring a 120 kb deletion in SHANK2 and two control lines from each parent, *Stem Cell Res.* 49 (2020), 102004.
- [45] C.S. Leblond, J. Heinrich, R. Delorme, C. Proepper, C. Betancur, G. Huguet, M. Konyukh, P. Chaste, E. Ey, M. Rastam, H. Anckarsater, G. Nygren, I. C. Gillberg, J. Melke, R. Toro, B. Regnault, F. Fauchereau, O. Mercati, N. Lemiere, D. Skuse, M. Poot, R. Holt, A.P. Monaco, I. Jarvela, K. Kantojarvi, R. Vanhala, S. Curran, D.A. Collier, P. Bolton, A. Chiochetti, S.M. Klauk, F. Poustka, C. M. Freitag, R. Waltes, M. Kopp, E. Duketis, E. Bacchelli, F. Minopoli, L. Ruta, A. Battaglia, L. Mazzone, E. Maestrini, A.F. Sequeira, B. Oliveira, A. Vicente, G. Oliveira, D. Pinto, S.W. Scherer, D. Zelenika, M. Delepine, M. Lathrop, D. Bonneau, V. Guinchat, F. Devillard, B. Assouline, M.C. Mouren, M. Leboyer, C. Gillberg, T.M. Boeckers, T. Bourgeron, Genetic and functional analyses of SHANK2 mutations suggest a multiple hit model of autism spectrum disorders, *PLoS Genet* 8 (2) (2012), e1002521.
- [46] S. Kim, Y.E. Kim, I. Song, Y. Ujihara, N. Kim, Y.H. Jiang, H.H. Yin, T.H. Lee, I. H. Kim, Neural circuit pathology driven by Shank3 mutation disrupts social behaviors, *Cell Rep.* 39 (10) (2022), 110906.
- [47] E. Lee, S. Lee, J.J. Shin, W. Choi, C. Chung, S. Lee, J. Kim, S. Ha, R. Kim, T. Yoo, Y. E. Yoo, J. Kim, Y.W. Noh, I. Rhim, S.Y. Lee, W. Kim, T. Lee, H. Shin, I.J. Cho, K. Deisseroth, S.J. Kim, J.M. Park, M.W. Jung, S.B. Paik, E. Kim, Excitatory synapses and gap junctions cooperate to improve Pv neuronal burst firing and cortical social cognition in Shank2-mutant mice, *Nat. Commun.* 12 (1) (2021) 5116.
- [48] D.H. Simmons, H.K. Titley, C. Hansel, P. Mason, Behavioral tests for mouse models of autism: an argument for the inclusion of cerebellum-controlled motor behaviors, *Neuroscience* 462 (2021) 303–319.
- [49] Y.C. Chang, T.B. Cole, L.G. Costa, Behavioral phenotyping for autism spectrum disorders in mice, *Curr. Protoc. Toxicol.* 72 (2017) 11 22 1–11 22 21.
- [50] J. Chabout, J. Jones-Macopson, E.D. Jarvis, Eliciting and analyzing male mouse ultrasonic vocalization (USV) songs, *J. Vis. Exp.* (123) (2017).
- [51] J. Fujino, S. Tei, T. Itahashi, Y. Aoki, H. Ohta, M. Kubota, M. Isobe, R. I. Hashimoto, M. Nakamura, N. Kato, H. Takahashi, Need for closure and cognitive flexibility in individuals with autism spectrum disorder: a preliminary study, *Psychiatry Res.* 271 (2019) 247–252.
- [52] S. Tei, J. Fujino, R.I. Hashimoto, T. Itahashi, H. Ohta, C. Kanai, M. Kubota, M. Nakamura, N. Kato, H. Takahashi, Inflexible daily behaviour is associated with the ability to control an automatic reaction in autism spectrum disorder, *Sci. Rep.* 8 (1) (2018) 8082.
- [53] A.Y. Hung, K. Putai, C. Sala, J.G. Valtschanoff, J. Ryu, M.A. Woodworth, F. L. Kidd, C.C. Sung, T. Miyakawa, M.F. Bear, R.J. Weinberg, M. Sheng, Smaller dendritic spines, weaker synaptic transmission, but enhanced spatial learning in mice lacking Shank1, *J. Neurosci.* 28 (7) (2008) 1697–1708.
- [54] A.O. Sungur, K.J. Vorckel, R.K. Schwarting, M. Wöhr, Repetitive behaviors in the Shank1 knockout mouse model for autism spectrum disorder: developmental aspects and effects of social context, *J. Neurosci. Methods* 234 (2014) 92–100.
- [55] A.O. Sungur, R.K. Schwarting, M. Wöhr, Early communication deficits in the Shank1 knockout mouse model for autism spectrum disorder: developmental aspects and effects of social context, *Autism Res* 9 (6) (2016) 696–709.
- [56] R. Kim, J. Kim, C. Chung, S. Ha, S. Lee, Y.E. Yoo, W. Kim, W. Shin, E. Kim, Cell-type-specific Shank2 deletion in mice leads to differential synaptic and behavioral phenotypes, *J. Neurosci.* 38 (17) (2018) 4076–4092.
- [57] C.S. Lim, H. Kim, N.K. Yu, S.J. Kang, T. Kim, H.G. Ko, J. Lee, J.E. Yang, H.H. Ryu, T. Park, J. Gim, H.J. Nam, S.H. Baek, S. Wegener, D. Schmitz, T.M. Boeckers, M. G. Lee, E. Kim, J.H. Lee, Y.S. Lee, B.K. Kaang, Enhancing inhibitory synaptic function reverses spatial memory deficits in Shank2 mutant mice, *Neuropharmacol.* 112(Pt A) (2017) 104–112.
- [58] H. Won, H.R. Lee, H.Y. Gee, W. Mah, J.I. Kim, J. Lee, S. Ha, C. Chung, E.S. Jung, Y.S. Cho, S.G. Park, J.S. Lee, K. Lee, D. Kim, Y.C. Bae, B.K. Kaang, M.G. Lee, E. Kim, Autistic-like social behaviour in Shank2-mutant mice improved by restoring NMDA receptor function, *Nature* 486 (7402) (2012) 261–265.
- [59] E. Ey, N. Torquet, A.M. Le Sourd, C.S. Leblond, T.M. Boeckers, P. Faure, T. Bourgeron, The autism ProSAP1/Shank2 mouse model displays quantitative and structural abnormalities in ultrasonic vocalisations, *Behav. Brain Res* 256 (2013) 677–689.
- [60] M.J. Schmeisser, E. Ey, S. Wegener, J. Bockmann, A.V. Stempel, A. Kuebler, A. L. Janssen, P.T. Udvardi, E. Shibani, C. Spilker, D. Balschun, B.V. Skryabin, S. Dieck, K.H. Smalla, D. Montag, C.S. Leblond, P. Faure, N. Torquet, A.M. Le Sourd, R. Toro, A.M. Grabrucker, S.A. Shoichet, D. Schmitz, M.R. Kreutz, T. Bourgeron, E.D. Gundelfinger, T.M. Boeckers, Autistic-like behaviours and hyperactivity in mice lacking ProSAP1/Shank2, *Nature* 486 (7402) (2012) 256–260.
- [61] X. Wang, Q. Xu, A.L. Bey, Y. Lee, Y.H. Jiang, Transcriptional and functional complexity of Shank3 provides a molecular framework to understand the phenotypic heterogeneity of SHANK3 causing autism and Shank3 mutant mice, *Mol. Autism* 5 (2014) 30.
- [62] O. Bozdagi, T. Sakurai, D. Papapetrou, X. Wang, D.L. Dickstein, N. Takahashi, Y. Kajiwara, M. Yang, A.M. Katz, M.L. Scattoni, M.J. Harris, R. Saxena, J. L. Silverman, J.N. Crawley, Q. Zhou, P.R. Hof, J.D. Buxbaum, Haploinsufficiency of the autism-associated Shank3 gene leads to deficits in synaptic function, social interaction, and social communication, *Mol. Autism* 1 (1) (2010) 15.
- [63] M. Yang, O. Bozdagi, M.L. Scattoni, M. Wöhr, F.I. Rouillet, A.M. Katz, D. N. Abrams, D. Kalikhman, H. Simon, L. Woldeyohannes, J.Y. Zhang, M.J. Harris, R. Saxena, J.L. Silverman, J.D. Buxbaum, J.N. Crawley, Reduced excitatory neurotransmission and mild autism-relevant phenotypes in adolescent Shank3 null mutant mice, *J. Neurosci.* 32 (19) (2012) 6525–6541.
- [64] T.C. Jaramillo, H.E. Speed, Z. Xuan, J.M. Reimers, S. Liu, C.M. Powell, Altered striatal synaptic function and abnormal behaviour in Shank3 Exon4-9 Deletion Mouse Model of Autism, *Autism Res* 9 (3) (2016) 350–375.
- [65] J. Lee, C. Chung, S. Ha, D. Lee, D.Y. Kim, H. Kim, E. Kim, Shank3-mutant mice lacking exon 9 show altered excitation/inhibition balance, enhanced rearing, and spatial memory deficit, *Front Cell Neurosci.* 9 (2015) 94.
- [66] M. Kouser, H.E. Speed, C.M. Dewey, J.M. Reimers, A.J. Widman, N. Gupta, S. Liu, T.C. Jaramillo, M. Bangash, B. Xiao, P.F. Worley, C.M. Powell, Loss of predominant Shank3 isoforms results in hippocampus-dependent impairments in behavior and synaptic transmission, *J. Neurosci.* 33 (47) (2013) 18448–18468.
- [67] H.E. Speed, M. Kouser, Z. Xuan, J.M. Reimers, C.F. Ochoa, N. Gupta, S. Liu, C. M. Powell, Autism-associated insertion mutation (InsG) of Shank3 Exon 21 causes impaired synaptic transmission and behavioral deficits, *J. Neurosci.* 35 (26) (2015) 9648–9665.
- [68] T.C. Jaramillo, H.E. Speed, Z. Xuan, J.M. Reimers, C.O. Escamilla, T.P. Weaver, S. Liu, I. Filonova, C.M. Powell, Novel Shank3 mutant exhibits behaviors with face validity for autism and altered striatal and hippocampal function, *Autism Res* 10 (1) (2017) 42–65.
- [69] Y. Zhou, T. Kaiser, P. Monteiro, X. Zhang, M.S. Van der Goes, D. Wang, B. Barak, M. Zeng, C. Li, C. Lu, M. Wells, A. Amaya, S. Nguyen, C.F. Ochoa, N. Sanjana, Y. Zhou, M. Zhang, F. Zhang, Z. Fu, G. Feng, Mice with Shank3 mutations associated with ASD and schizophrenia display both shared and distinct defects, *Neuron* 89 (1) (2016) 147–162.
- [70] X. Wang, A.L. Bey, B.M. Katz, A. Badea, N. Kim, L.K. David, L.J. Duffney, S. Kumar, S.D. Mague, S.W. Hulbert, N. Dutta, V. Hayrapetyan, C. Yu, E. Gaidis, S. Zhao, J.D. Ding, Q. Xu, L. Chung, R.M. Rodriguiz, F. Wang, R.J. Weinberg, W. C. Wetsel, K. Dzirasa, H. Yin, Y.H. Jiang, Altered mGluR5-Homer scaffolds and corticostriatal connectivity in a Shank3 complete knockout model of autism, *Nat. Commun.* 7 (2016) 11459.
- [71] T. Yoo, H. Cho, J. Lee, H. Park, Y.E. Yoo, E. Yang, J.Y. Kim, H. Kim, E. Kim, GABA Neuronal Deletion of Shank3 Exons 14-16 in Mice Suppresses Striatal Excitatory Synaptic Input and Induces Social and Locomotor Abnormalities, *Front Cell Neurosci.* 12 (2018) 341.
- [72] T. Yoo, H. Cho, H. Park, J. Lee, E. Kim, Shank3 exons 14-16 deletion in glutamatergic neurons leads to social and repetitive behavioral deficits associated with increased cortical layer 2/3 neuronal excitability, *Front Cell Neurosci.* 13 (2019) 458.
- [73] Y.E. Yoo, T. Yoo, S. Lee, J. Lee, D. Kim, H.M. Han, Y.C. Bae, E. Kim, Shank3 mice carrying the human Q321R mutation display enhanced self-grooming, abnormal electroencephalogram patterns, and suppressed neuronal excitability and seizure susceptibility, *Front Mol. Neurosci.* 12 (2019) 155.
- [74] Y. Mei, P. Monteiro, Y. Zhou, J.A. Kim, X. Gao, Z. Fu, G. Feng, Adult restoration of Shank3 expression rescues selective autistic-like phenotypes, *Nature* 530 (7591) (2016) 481–484.
- [75] W. Wang, C. Li, Q. Chen, M.S. van der Goes, J. Hawrot, A.Y. Yao, X. Gao, C. Lu, Y. Zhang, Q. Zhang, K. Lyman, D. Wang, B. Guo, S. Wu, C.R. Gerfen, Z. Fu, G. Feng, Striatopallidal dysfunction underlies repetitive behavior in Shank3-deficient model of autism, *J. Clin. Invest* 127 (5) (2017) 1978–1990.
- [76] C. Vicidomini, L. Ponzoni, D. Lim, M.J. Schmeisser, D. Reim, N. Morello, D. Orellana, A. Tozzi, V. Durante, P. Scalmani, M. Mantegazza, A.A. Genazzani, M. Giustetto, M. Sala, P. Calabresi, T.M. Boeckers, C. Sala, C. Verpelli, Pharmacological enhancement of mGlu5 receptors rescues behavioral deficits in SHANK3 knock-out mice, *Mol. Psychiatry* 22 (5) (2017) 689–702.
- [77] C. Balaan, M.J. Corley, T. Eulalio, K. Leite-Ahyo, A.P.S. Pang, R. Fang, V. S. Khadka, A.K. Maunakea, M.A. Ward, Juvenile Shank3b deficient mice present with behavioral phenotype relevant to autism spectrum disorder, *Behav. Brain Res* 356 (2019) 137–147.
- [78] A.L. Bey, X. Wang, H. Yan, N. Kim, R.L. Passman, Y. Yang, X. Cao, A.J. Towers, S. W. Hulbert, L.J. Duffney, E. Gaidis, R.M. Rodriguiz, W.C. Wetsel, H.H. Yin, Y. H. Jiang, Brain region-specific disruption of Shank3 in mice reveals a dissociation for cortical and striatal circuits in autism-related behaviors, *Transl. Psychiatry* 8 (1) (2018) 94.
- [79] B. Guo, J. Chen, Q. Chen, K. Ren, D. Feng, H. Mao, H. Yao, J. Yang, H. Liu, Y. Liu, F. Jia, C. Qi, T. Lynn-Jones, H. Hu, Z. Fu, G. Feng, W. Wang, S. Wu, Anterior cingulate cortex dysfunction underlies social deficits in Shank3 mutant mice, *Nat. Neurosci.* 22 (8) (2019) 1223–1234.
- [80] A. Mossa, J. Pagano, L. Ponzoni, A. Tozzi, E. Vezzoli, M. Sciacaluga, C. Costa, S. Beretta, M. Francolini, M. Sala, P. Calabresi, T.M. Boeckers, C. Sala, C. Verpelli, Developmental impaired Akt signaling in the Shank1 and Shank3 double knock-out mice, *Mol. Psychiatry* (2021).
- [81] V. Echeverria, R. Zeitlin, S. Burgess, S. Patel, A. Barman, G. Thakur, M. Mamcarz, L. Wang, D.B. Sattelle, D.A. Kirschner, T. Mori, R.M. Leblanc, R. Prabhakar, G. W. Arendash, Cotinine reduces amyloid-beta aggregation and improves memory in Alzheimer's disease mice, *J. Alzheimers Dis.* 24 (4) (2011) 817–835.
- [82] M. Pardo, E. Beurel, R.S. Jope, Cotinine administration improves impaired cognition in the mouse model of Fragile X syndrome, *Eur. J. Neurosci.* 45 (4) (2017) 490–498.
- [83] C. Cheroni, N. Caporale, G. Testa, Autism spectrum disorder at the crossroad between genes and environment: contributions, convergences, and interactions in ASD developmental pathophysiology, *Mol. Autism* 11 (1) (2020) 69.
- [84] C. Chung, W. Shin, E. Kim, Early and late corrections in mouse models of autism spectrum disorder, *Biol. Psychiatry* 91 (11) (2022) 934–944.
- [85] P. Karimi, E. Kamali, S.M. Mousavi, M. Karahmadi, Environmental factors influencing the risk of autism, *J. Res Med Sci.* 22 (2017) 27.

- [86] A. Massarali, D. Adhya, D.P. Srivastava, S. Baron-Cohen, M.R. Kotter, Virus-induced maternal immune activation as an environmental factor in the etiology of autism and schizophrenia, *Front Neurosci.* 16 (2022), 834058.
- [87] C. Pham, C. Symeonides, M. O'Hely, P.D. Sly, L.D. Knibbs, S. Thomson, P. Vuillermin, R. Saffery, A.L. Ponsonby, G. Barwon, Infant Study Investigator, Early life environmental factors associated with autism spectrum disorder symptoms in children at age 2 years: A birth cohort study, *Autism* (2022), 13623613211068223.
- [88] C.J. Tseng, C.J. McDougle, J.M. Hooker, N.R. Zurcher, Epigenetics of autism spectrum disorder: histone deacetylases, *Biol. Psychiatry* 91 (11) (2022) 922–933.
- [89] C. Chung, S. Ha, H. Kang, J. Lee, S.M. Um, H. Yan, Y.E. Yoo, T. Yoo, H. Jung, D. Lee, E. Lee, S. Lee, J. Kim, R. Kim, Y. Kwon, W. Kim, H. Kim, L. Duffney, D. Kim, W. Mah, H. Won, S. Mo, J.Y. Kim, C.S. Lim, B.K. Kaang, T.M. Boeckers, Y. Chung, H. Kim, Y.H. Jiang, E. Kim, Early correction of N-methyl-D-aspartate receptor function improves autistic-like social behaviors in adult shank2(-/-) mice, *Biol. Psychiatry* 85 (7) (2019) 534–543.
- [90] T.C. Jaramillo, Z. Xuan, J.M. Reimers, C.O. Escamilla, S. Liu, C.M. Powell, Early restoration of Shank3 expression in shank3 knock-out mice prevents core ASD-like behavioral phenotypes, *eNeuro* 7 (3) (2020).
- [91] L. Qin, K. Ma, Z.J. Wang, Z. Hu, E. Matas, J. Wei, Z. Yan, Social deficits in Shank3-deficient mouse models of autism are rescued by histone deacetylase (HDAC) inhibition, *Nat. Neurosci.* 21 (4) (2018) 564–575.
- [92] W.J. Bian, C.L. Brewer, J.A. Kauer, L. de Lecea, Adolescent sleep shapes social novelty preference in mice, *Nat. Neurosci.* (2022).
- [93] K.J. Parker, Leveraging a translational research approach to drive diagnostic and treatment advances for autism, *Mol. Psychiatry* 27 (6) (2022) 2650–2658.
- [94] J. Li, W. Zhang, H. Yang, D.P. Howrigan, B. Wilkinson, T. Souaiaia, O. V. Evgrafov, G. Genovese, V.A. Clementel, J.C. Tudor, T. Abel, J.A. Knowles, B. M. Neale, K. Wang, F. Sun, M.P. Coba, Spatiotemporal profile of postsynaptic interactomes integrates components of complex brain disorders, *Nat. Neurosci.* 20 (8) (2017) 1150–1161.
- [95] B. Wilkinson, O.V. Evgrafov, D. Zheng, N. Hartel, J.A. Knowles, N.A. Graham, J. K. Ichida, M.P. Coba, Endogenous cell type-specific disrupted in schizophrenia 1 interactomes reveal protein networks associated with neurodevelopmental disorders, *Biol. Psychiatry* 85 (4) (2019) 305–316.
- [96] Y. Xu, X. Song, D. Wang, Y. Wang, P. Li, J. Li, Proteomic insights into synaptic signaling in the brain: the past, present and future, *Mol. Brain* 14 (1) (2021) 37.
- [97] H. Kim, B. Cho, H. Park, J. Kim, S. Kim, J. Shin, C.J. Lengner, K.J. Won, J. Kim, Dormant state of quiescent neural stem cells links Shank3 mutation to autism development, *Mol. Psychiatry* (2022).
- [98] A.A. Coley, W.J. Gao, PSD95: A synaptic protein implicated in schizophrenia or autism? *Prog. Neuropsychopharmacol. Biol. Psychiatry* 82 (2018) 187–194.
- [99] D.S. Roy, Y. Zhang, T. Aida, S. Choi, Q. Chen, Y. Hou, N.E. Lea, K.M. Skaggs, J. C. Quay, M. Liew, H. Maisano, V. Le, C. Jones, J. Xu, D. Kong, H.A. Sullivan, A. Saunders, S.A. McCarroll, I.R. Wickersham, G. Feng, Anterior thalamic dysfunction underlies cognitive deficits in a subset of neuropsychiatric disease models, *Neuron* 109 (16) (2021) 2590–2603 e13.
- [100] L. Rylaarsdam, A. Guemez-Gamboa, Genetic causes and modifiers of autism spectrum disorder, *Front Cell Neurosci.* 13 (2019) 385.